

UNIVERSITY OF GHANA

COLLEGE OF BASIC AND APPLIED SCIENCES

**ESTIMATION OF CONTRALATERAL BREAST DOSE FOR TANGENTIAL
BREAST IRRADIATION USING GAFCHROMIC FILM EBT2**

BY

**EMMANUEL YAW BOAMAH
(10508610)**

**THIS THESIS IS SUBMITTED TO THE UNIVERSITY OF GHANA, LEGON
IN PARTIAL FULFILLMENT OF THE REQUIREMENT FOR THE AWARD
OF MPhil MEDICAL PHYSICS DEGREE**

**DEPARTMENT OF MEDICAL PHYSICS, SCHOOL OF NUCLEAR AND
ALLIED SCIENCES**

JULY, 2016

DECLARATION

This thesis is the result of research work undertaken by Emmanuel Yaw Boamah in the Department of Medical Physics, University of Ghana, under the supervision of Prof. J.H Amuasi, Dr Francis Hasford and Mr. Samuel Tagoe.

I hereby declare that this thesis is the result of my own original research and that no part of it has been presented for another degree in this University or elsewhere. Duly other works and/or researches done by other researchers cited in this work have been acknowledged under references.

.....
EMMANUEL YAW BOAMAH
(STUDENT)

Date

.....
PROF. J.H AMUASI
(PRINCIPAL SUPERVISOR)

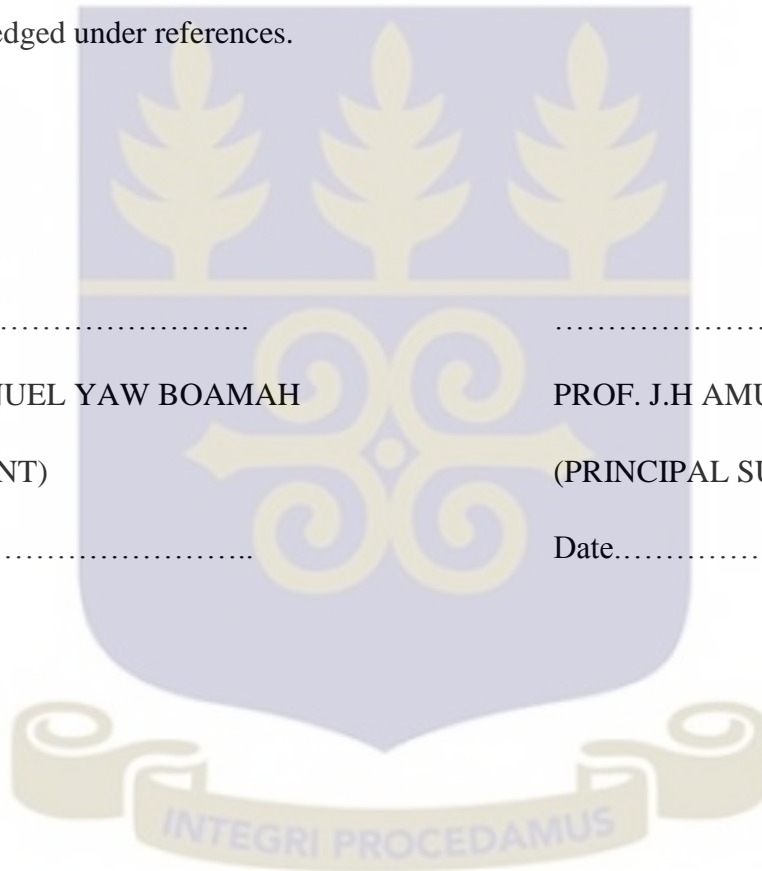
Date.....

.....
DR FRANCIS HASFORD
(CO-SUPERVISOR)

Date

.....
MR SAMUEL TAGOE
(CO-SUPERVISOR)

Date.....



DEDICATION

I dedicate this work to my mother Madam Veronica Serensuo, my uncle Chief Inspector Owusu Andrews, my cousin Mr Baffoe Paul and my siblings. Thank you for always being there for me.



ACKNOWLEDGEMENT

My profound gratitude to God Almighty whose abundant grace and mercies have seen me through this work.

I wish to express my heartfelt gratitude to my supervisors, Prof J.H Amuasi, Dr Francis Hasford, Mr Samuel Tagoe for their tremendous and outstanding hard work, patience, words of encouragement and motivation, constructive suggestions and guidance in the preparation of this thesis.

I am also grateful to Mr George Felix and Mr Philip Opong Junior of Sweden Ghana Medical Center, Mr Sassu of Korle-Bu Teaching hospitals for their selfless effort during gathering of data for this study.

My colleagues of 2016 medical physics class, may God bless you all for your company throughout our studies.

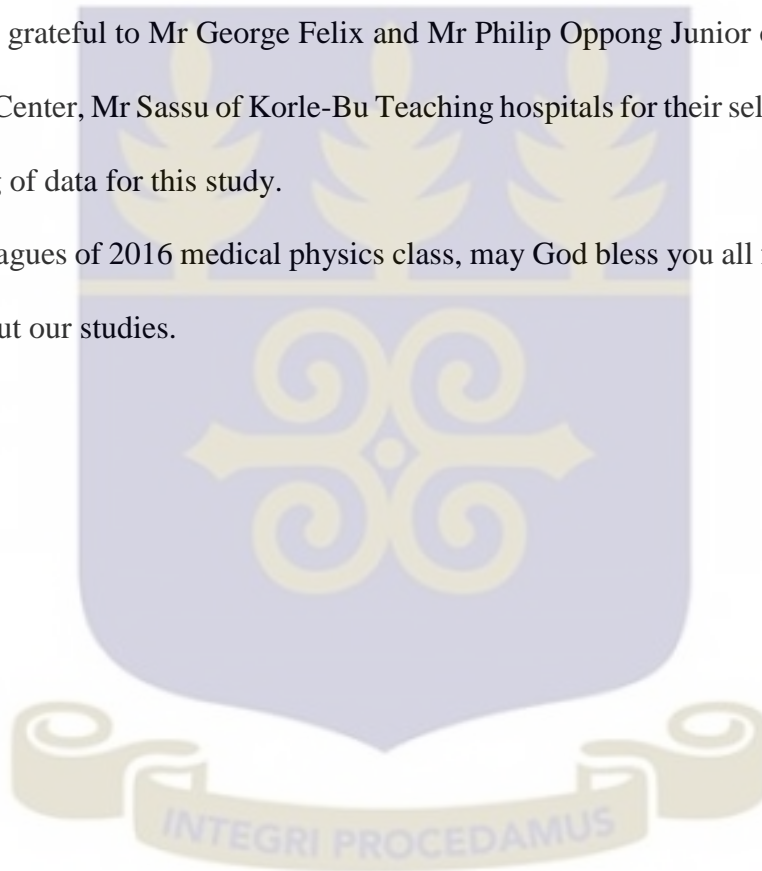


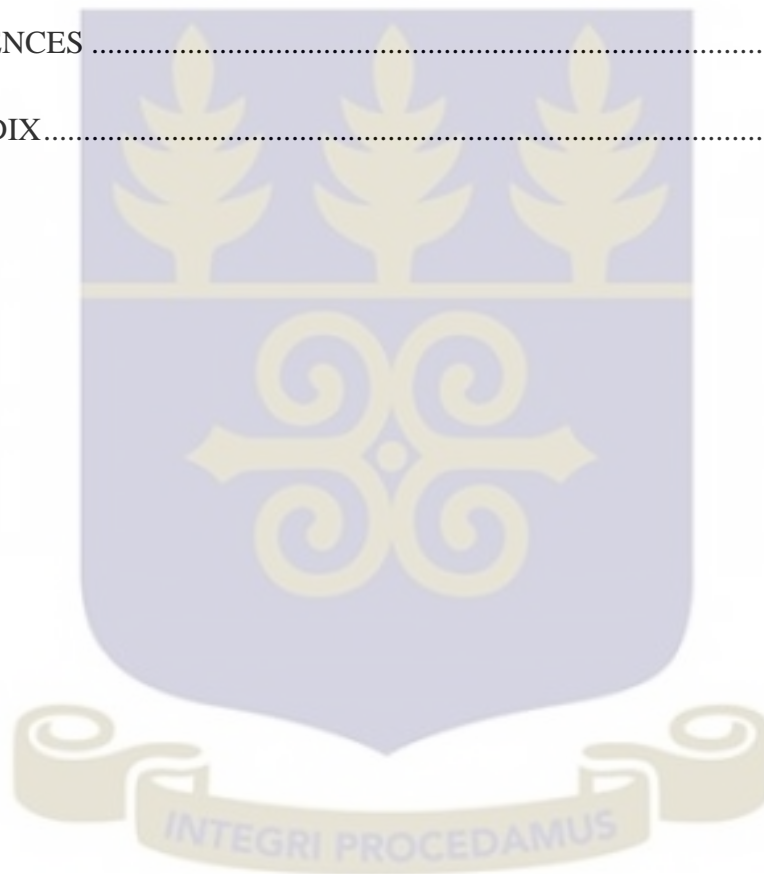
TABLE OF CONTENTS

DECLARATION	ii
DEDICATION	iii
ACKNOWLEDGEMENT	iv
TABLE OF CONTENTS	v
LIST OF TABLES	ix
LIST OF FIGURES	x
LIST OF PLATES	xi
LIST OF ABBREVIATIONS	xii
ABSTRACT	xiv
CHAPTER ONE	1
INTRODUCTION	1
1.0 Overview	1
1.1 Background	1
1.2 Problem Statement	3
1.3 Objectives of the study	4
1.4 Relevance and justification	5
1.5 Scope and limitation	5
1.6 Organization of thesis	5
CHAPTER TWO	7

LITERATURE REVIEW	7
2.0. Introduction	7
2.1. Radiation Therapy	7
2.1.1. Three-Dimensional Conformal Radiotherapy (3-DCRT).....	8
2.1.2. Treatment Planning Systems	11
2.1.3 Treatment Techniques of Radiotherapy	13
2.2 Volume Definition.....	15
2.2.1 Gross Tumour Volume (GTV)	16
2.2.2 Clinical Target Volume (CTV).....	16
2.2.3 Internal Target Volume (ITV)	17
2.2.4 Planning Target Volume (PTV)	17
2.3 The Organs at Risk and Radiation Tolerance Doses.....	18
2.3.1 Dose-Volume Constraints of contralateral breast.....	19
2.4 Peripheral Dose	19
2.5 Risk of Contralateral Breast Cancer.....	20
2.6 Radiation Dosimeters	21
2.6.1 Radiochromic Films	22
2.7. Multileaf Collimators (MLC).....	31
2.8. Wedges	33
CHAPTER THREE	38
MATERIALS AND METHOD	38

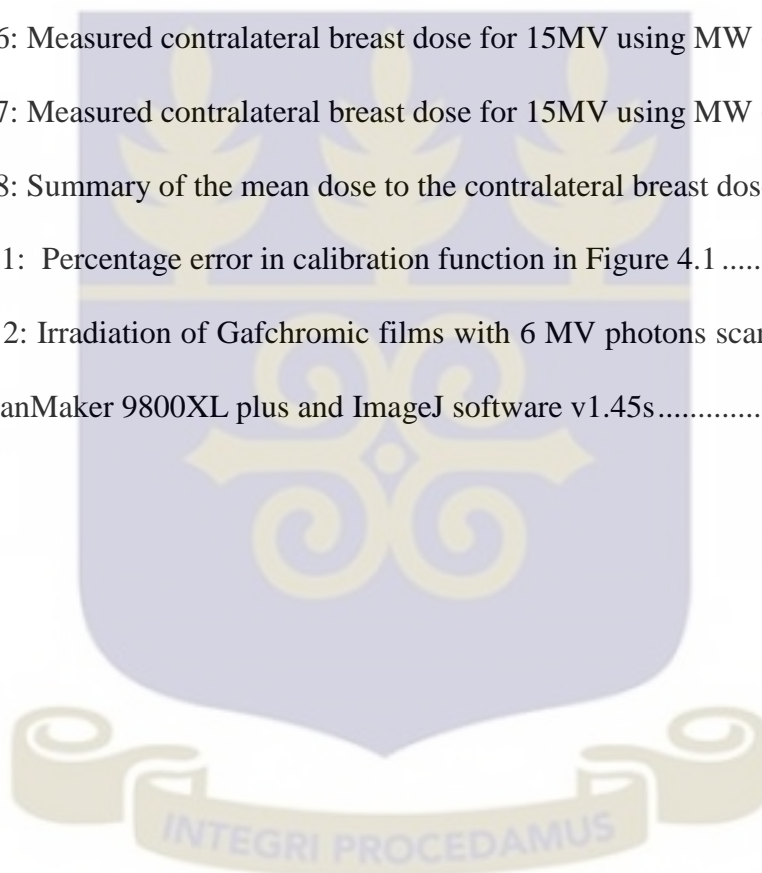
3.0 Introduction	38
3.1 Materials.....	38
3.1.1 Elekta Linear Accelerator unit.....	38
3.1.2 Gafchromic film (EBT2)	39
3.1.3 Rando Alderson Phantom.....	40
3.1.4 Mini Water Phantom	41
3.1.5 ScanMaker 9800XL Plus.....	42
3.2 Experimental Method.....	43
3.2.1 Calibration and irradiation procedures of Gafchromic EBT2 films	43
3.2.2 Planning Computed Tomography.....	44
3.2.3 Treatment planning.....	45
3.2.4 Measurement of contralateral breast dose using Gafchromic EBT2 film. ..	46
CHAPTER FOUR.....	50
RESULTS AND DISCUSSION	50
4.0 Introduction	50
4.1 Calibration curve.....	50
4.2 Results	53
4.3 Discussion	56
4.3.1 Measured contralateral breast doses	56
4.3.2 Effect of beam energy on contralateral breast dose.....	58
4.3.3 Effect of wedge (MW) on contralateral breast dose.....	60

CHAPTER FIVE	63
CONCLUSION AND RECOMMENDATIONS	63
5.0. Overview	63
5.1 Conclusion.....	63
5.2 Recommendations	64
5.3 Further study	65
REFERENCES	66
APPENDIX.....	76



LIST OF TABLES

Table 4. 1: Irradiation of Gafchromic films with 6 MV photons scanned and read out by the ScanMaker 9800XL plus and ImageJ software v1.45s.....	51
Table 4. 2: Measured contralateral breast dose for 6 MV using MW (15°).....	53
Table 4. 3: Measured contralateral breast dose for 6 MV using MW (30°).....	54
Table 4. 4: Measured contralateral breast dose for 6 MV using MW (60°).....	54
Table 4. 5: Measured contralateral breast dose for 15MV using MW (15°).....	55
Table 4. 6: Measured contralateral breast dose for 15MV using MW (30°).....	55
Table 4. 7: Measured contralateral breast dose for 15MV using MW (60°).....	56
Table 4. 8: Summary of the mean dose to the contralateral breast dose.....	59
Table A. 1: Percentage error in calibration function in Figure 4.1	76
Table A. 2: Irradiation of Gafchromic films with 6 MV photons scanned and read out by the ScanMaker 9800XL plus and ImageJ software v1.45s.....	77



LIST OF FIGURES

Figure 2. 1: 3D conformal EBRT Target Volume Construction 10

Figure 2. 2: Graphical representation of the volumes-of-interest, as defined by the ICRU 50 and 62 reports [2, 3] 16

Figure 2. 3: Configuration of GAFCHROMIC EBT2 Film [45].....24

Figure 2. 4: Energy Dependence of GAFCHROMIC EBT2 Dosimetry Film [46]26

Figure 2. 5: Net optical density versus dose for EBT2 film. The film was calibrated at 25 keV (circles), 30 keV (triangles), 35 keV (filled squares) and 4 MV (hollow squares) [35].....27

Figure 2. 6: GafChromic EBT2 film response curve over 10cm² [57]30

Figure 2. 8: Isodose curves for a wedged 6 MV photon beam. The isodoses have been normalized to Z_{max} with the wedge in place [54].34

Figure 2. 9: Conformal radiotherapy with wedges (CRT-W) technique: a) Transverse slice of CRT-W. b) Dose volume histogram (DVH): pink colour: PTV, green colour: ipsilateral lung, brown colour: heart, light green colour: LAD and magenta colour: contralateral breast. c) Frontal slice of CRT-W. d) Sagittal slice of CRT-W. [80].....35

Figure 2. 11: Principle of the EDW [80].....37

Figure 4. 1: Calibration curves of EBT2 films read out using ImageJ software52

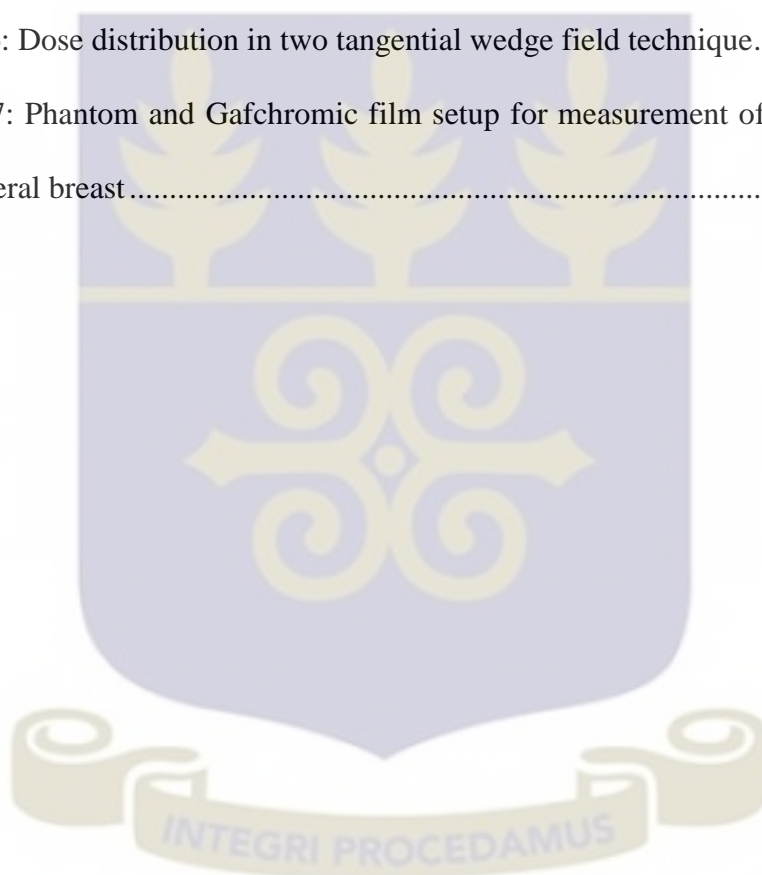
Figure 4. 2: Comparison of beam energy on contralateral breast dose.....60

Figure 4. 3: comparison of contralateral breast dose for MW (15°), MW (30°) and MW (60°) using 6 MV photon beam.....61

Figure 4. 4: comparison of contralateral breast dose for MW (15°), MW (30°) and MW (60°) using 15MV photon beam62

LIST OF PLATES

Plate 3. 1: Elekta Linear Accelerator unit	39
Plate 3. 2: 1 cm × 1.5 cm pieces of Gafchromic EBT2 film.....	40
Plate 3. 3: An anthropomorphic female Rando phantom.....	41
Plate 3. 4: Mini water phantom.....	42
Plate 3. 5: Images of CT scan of the Rando Alderson female anthropomorphic phantom	45
Plate 3. 6: Dose distribution in two tangential wedge field technique.....	46
Plate 3. 7: Phantom and Gafchromic film setup for measurement of the doses on the contralateral breast.....	48



LIST OF ABBREVIATIONS

KBTH	Korle Bu teaching Hospital
MPhil	Master of Philosophy
SGMC	Sweden Ghana Medical Center
MV	Mega Voltage
PMMA	Polymethylmetacrylate
SSD	Source to surface distance
SAD	Source to axis distance
MLC	Multileaf collimator
ICRU	International Commission on Radiation Units and Measurements
ICRP	International Commission on Radiological Protection
IAEA	International Atomic Energy Agency
TECDOC	Technical Documentation
TG	Task Group
RTOG	Radiation Therapy Oncology Group
OAR	Organ at risk
3-D	Three Dimensional
2-D	Two Dimensional
3DCRT	Three-dimensional conformal radiation therapy
CBC	Contralateral Breast Cancer
IMRT	Intensity modulated radiotherapy
EBRT	External beam radiotherapy
RGB	Red green blue
CT	Computed tomography
MW	Motorized wedge
MU	Monitor unit
TBV	Target breast volume
TPS	Treatment planning system
DVHs	Dose volume histograms
TCP	Tumour control probability

NTCP	Normal tissue complication probability
CTV	Clinical target volume
GTV	Gross tumour volume
PTV	Planning target volume
BEV	Beam-eye-view
ITV	Internal target volume
RT	Radiotherapy
ISP	International specialty products
OD	Optical density
MCNP	Monte Carlo Non-Particle
EDW	Enhanced dynamic wedges
ROI	Region of interest
CC	Collapsed cone
CRT-W	Conformal radiotherapy with wedges
DP	Dose point
SI	Superior inferior
ML	Medial lateral



ABSTRACT

The dose to the contralateral breast for tangential breast irradiation has been estimated using Gafchromic films EBT2. The data collected consisted of measurements taken with anthropomorphic female Rando phantom. The EBT2 films were scanned and read using ScanMaker 9800XL plus and ImageJ software. A calibration curve was constructed using fourth – order polynomial fit to the data and a calibration equation was obtained from the graph which was used to convert the grey values into doses. Comparison of dose to the contralateral breast using different wedge angles and different photon beam energies has been done. The mean dose to the contralateral breast recorded were 1.93 Gy and 3.14 Gy for 6 MV and 15 MV photon beams respectively. The results show that the mean dose to the contralateral breast for 6 MV using 60^o motorised wedge produced higher surface dose to the contralateral breast than 30^o and 15^o wedges respectively. Similarly the mean dose to the contralateral breast for 15 MV using 60^o motorised wedge produced higher surface dose to the contralateral breast than 30^o and 15^o wedges respectively. Results from this study show that the dose to the contralateral breast increases with increasing wedge angle. Analysis of the results from the 6 MV and 15 MV shows that the 15MV photon beam produced a higher doses to the contralateral breast as compared with the 6 MV photon beam by 6.42%.

CHAPTER ONE

INTRODUCTION

1.0 Overview

This chapter presents the background, relevance and justification, statement of the problem, the scope and objectives of the research work and the structure of the thesis.

1.1 Background

Cancer patients commonly receive a combination of treatments that may include surgery, chemotherapy and radiotherapy. In radiotherapy ionizing radiations are used to cure the disease or alleviate pain. The optimal therapeutic effect of radiotherapy is achieved when cancer cells are eradicated while normal tissue damage is kept to a minimum [1]. The two types of radiotherapy are external beam radiotherapy and brachytherapy. Brachytherapy is the short distance treatment of cancer with radiation from small encapsulated radionuclide sources. This thesis is focused on external beam radiotherapy (EBRT).

In external beam radiotherapy (EBRT) a beam or several beams of high-energy x-rays are delivered to a patient's tumour. The beams are generated outside the patient (usually by a linear accelerator) and are targeted at the tumour site. These high energy x-rays can deposit their dose to the area of the tumour to destroy the cancer cells and, with careful treatment planning, spare the surrounding normal tissues. No radioactive sources are placed inside the patient's body. The procedure may be performed before or after surgery to remove a cancerous tumour, to reduce the tumour size before surgery, or to prevent the tumour from coming back after surgery. Three-dimensional conformal radiation therapy (3D-CRT) and Intensity Modulated Radiotherapy (IMRT) improve

the relationship between the likelihood of tumour control and the probability of adjacent normal tissue complications [21]. Three-dimensional conformal radiation therapy (3D-CRT) delivers radiation beams shaped like the tumour at the cancer from different directions. Patients are fitted with a mould or cast to keep the body part still so the radiation can be aimed very accurately. This may make it possible to reduce radiation damage to normal tissues and better kill the cancer by increasing the radiation dose to the tumour [23].

External photon beam radiotherapy is usually carried out with more than one radiation beam in order to achieve a uniform dose distribution inside the target volume and as low as possible a dose in healthy tissues surrounding the target. ICRU Report No. 50 [2] recommends a target dose uniformity within +7% and -5% of the dose delivered to a well-defined prescription point within the target. Modern photon beam radiotherapy is carried out with a variety of beam energies and field sizes under one of two set-up conventions: a constant source to surface distance (SSD) for all beams or an isocentric set-up with a constant source to axis distance (SAD) [1]. External beam therapy is used to treat the following diseases: breast cancer, colorectal (Bowel) cancer, oesophageal cancer, head and neck cancer, lung cancer, prostate cancer and brain tumour as well as many others.

Breast cancer is the most common cancer among women, worldwide. It is becoming number one killer in females. Therefore it has become an increasingly important subject of research all over the world. Globally, every 3 minutes a woman is diagnosed with breast cancer, amounting to one million cases annually. According to World Cancer Report, the incidence could go up by 50% to 1.5 million by 2020 [8, 9].

Contralateral breast cancer (CBC) is the most common secondary malignancy in patients treated for first breast cancer, and it accounts for about 50% of all second primary cancers [15]. Their incidence rates at 5, 10, 15 and 20 years are 3.5%, 7.6%, 11.3% and 15.4% respectively, with the median diagnosis time being 8.2 years [22]. Some researches revealed that patients who were under 45 years of age treated with breast irradiation had an elevated risk of developing CBC than the counterparts with no radiotherapy treatment [15, 17, 18].

Breast cancer is most curable when detected at its earlier stages. Radiotherapy plays an important role in the treatment of breast cancer and several studies have shown better survival of patients after mastectomy followed by radiotherapy [10]. Women with breast cancer have three-to four-fold increased risk of developing a new primary cancer in the contralateral breast, as compared with the risk of a first/primary breast cancer among other women [11].

1.2 Problem Statement

During external beam radiotherapy of malignant breast, the contralateral breast receives radiation due to leakage from treatment gantry, scatter radiation from the secondary collimators and beam modifiers such as wedges and MLC. Such dose outside the geometric boundaries of the treatment fields is known as peripheral dose. Therefore, the peripheral dose delivered to some anatomical structures with high radiation sensitivity such as the contralateral breast, is of great concern. Studies have shown that the scatter radiation to the contralateral breast may play a large part in the induction of second breast cancer [24, 25]. Breast is highly radiosensitive tissue for radiation induced second malignancy and is of more concern for female younger than 45 years

of age receiving radiotherapy for breast malignancy. Several investigators, [12-14] who have measured the contralateral breast dose on an Anderson Rando phantom observed that the scatter dose to contralateral breast during medial, tangential and supraclavicular field is quite high and sometimes of the order of 500 cGy for 5000 cGy primary breast dose. Therefore the quantification of the contralateral breast especially during treatment of diseased breast by external beam is very important. In the present study, measurement of contralateral breast dose was done by using Gafchromic EBT2 radiochromic dosimetry film because it has high spatial resolution and it provides larger area for dosimetry. Also the weak energy dependence of the EBT2 makes it most suitable for clinical use compared to other films [30].

1.3 Objectives of the study

The primary objective of the study is to estimate the dose delivered to the contralateral breast for tangential breast irradiation in three dimensional conformal radiation therapy breast irradiation using Gafchromic film EBT2.

The specific objectives of the study are

- i) To investigate and compare the dose to contralateral breast using different wedge angles.
- ii) To investigate the alteration of contralateral breast dose using different beam energies

1.4 Relevance and justification

External beam radiotherapy is being used regularly to treat the breast malignancy postoperatively. Estimation of the dose to the contralateral breast for primary breast irradiation is helpful to evaluate the risk of radiation induced secondary breast malignancy

Obtaining a better understanding of the potential increase, or decrease, in dose to target and normal tissues could facilitate a better understanding of the risks associated with external beam treatment techniques.

Detailed knowledge of the dose to the contralateral breast is necessary to assess the potential risk that may exist for the induction of secondary cancer and also to determine ways of reducing the magnitude of this dose so as to minimize further any possible risk.

1.5 Scope and limitation

The scope of this thesis is in the area of 3D conformal external beam radiotherapy, and particularly the dose to the contralateral breast that results from the use of different beam energies and wedge angles. The dose measurements in the contralateral breast were taken with Elekta Synergy 11 treatment machine using Anderson female Rando phantom and Gafchromic EBT2 films.

1.6 Organization of thesis

This thesis is organized as follows. Chapter one is an introduction to the research and provides an overview of the current state of knowledge relevant to the study. Chapter two reviews existing literature relevant to the research problem. Chapter three focuses on the experimental and theoretical framework of the study. The results obtained are

presented and discussed in chapter four. Chapter five contains the conclusion of the study, recommendations and suggestions for further research.



CHAPTER TWO

LITERATURE REVIEW

2.0. Introduction

This chapter contains literature, articles and publications of materials relevant to this research study.

2.1. Radiation Therapy

Radiation and radioactivity were discovered over a century ago by a German physicist Wilhelm Roentgen in 1895 and Henry Becquerel in 1876 respectively. Today, radiation is an important part of cancer treatment of which more than half of all people with cancer get radiation either as part of their primary treatment or in connection with recurrences or palliation [44]. To this point radiotherapy is defined as a branch of medicine that deals with the treatment of tumour and other malignant tissues through ionizing radiations. The aim of radiation therapy is to tailor a tumouricidal dose envelope to a target volume and to deliver as low as a possible radiation dose to all other normal tissues. There are two types of radiotherapy; external beam radiotherapy and brachytherapy. External beam radiotherapy where the source of radiation, is placed outside the patient and beams of radiation are delivered to a specific area of the patient's body. This method is called 3-Dimensional Conformal Radiotherapy (3DCRT). The target or tumour volume (the disease) is modelled and the radiations are directed to this volume. Therefore the dose of radiations hitting the healthy cells of the anatomically adjacent organs, which are not affected by the illness, can be reduced. Brachytherapy on the other hand is where a radioactive source is placed in direct contact or close proximity to the target or tumour volume. The radioactive material used in

brachytherapy comes in different shapes and sizes which include wires, capsules or spheres [58]. Interstitial and intravascular radiation are the two main types of brachytherapy. Interstitial is when the radiation source is placed directly into or next to the tumour using small pellets, seeds, wires, tubes, or containers. In intravascular radiation, a container of radioactive material is placed in a cavity of the body such as the chest, rectum, uterus, or vagina. Ultrasound, x-rays, or CT scans are used as guides in putting the radioactive source in the right place. The placement can be permanent or temporary. The radioactive source can be placed either in the pathological tissues or nearby and then removed after some time and this is known as brachytherapy with temporary implant. The situation in which the radioactive material is permanently left in place is known as brachytherapy with permanent implants [58].

2.1.1. Three-Dimensional Conformal Radiotherapy (3-DCRT)

The wide application of powerful computers in radiotherapy has made a substantial impact on treatment planning and delivery. 3-D CRT is now increasingly being practiced worldwide. 3-D CRT treatments are based on 3-D anatomic information and use dose distributions that conform as closely as possible to the target volume in terms of adequate dose to the tumour and minimum possible dose to normal tissue [59]. The concept of conformal dose distribution has also been extended to include clinical objectives such as maximizing tumour control probability (TCP) and minimizing normal tissue complication probability (NTCP). Thus, the 3-D CRT technique encompasses both the physical and biologic rationales in achieving the desired clinical results. Although 3-D CRT calls for optimal dose distribution, there are many obstacles to achieving these objectives. The major limitation is the knowledge of the tumour extent [59]. Depending on the invasive capacity of the disease, what is imaged is usually

not the CTV. It may be what is called the gross tumour volume (GTV). Thus, if the CTVs drawn on the cross-sectional images do not fully include the microscopic spread of the disease, the 3-D CRT loses its meaning of being conformal. If any part of the diseased tissue is missed or seriously under dosed, it will inevitably result in failure despite all the care and effort expended in treatment planning, treatment delivery, and quality assurance [59]. From the TCP point of view, accuracy in localization of CTV is more critical in 3-D CRT than in techniques that use generously wide fields and simpler beam arrangements to compensate for the uncertainty in tumour localization. Patient motion, including that of tumour volume, critical organs and external fiducial marks during imaging, simulation, and treatment, can give rise to systematic as well as random errors that must be accounted for when designing the planning target volume (PTV). If sufficient margins have been allowed for in the localization of PTV, the beam apertures are then shaped to conform and adequately cover the PTV (e.g., within 95% to 105% isodose surface relative to prescribed dose) [59]. Consideration must be given to the cross-beam profile, penumbra, and lateral radiation transport as a function of depth, radial distance, and tissue density in the design of conformal fields to adequately treat the PTV. Sufficient margins must be given between the PTV outline and the field boundary to ensure adequate dose to PTV at every treatment session. Even if the fields have been optimally designed, biologic response of the tumour and the normal tissues needs to be considered in achieving the goals of 3-D CRT [59]. In other words, the optimization of a treatment plan has to be evaluated not only in terms of dose distribution (e.g., dose volume histograms) but also in terms of dose-response characteristics of the given disease and the irradiated normal tissues. Various models involving TCP and NTCP have been proposed, but the clinical data to validate these models are scarce. Until more reliable data are available, caution is needed in using

these concepts to evaluate treatment plans. This is especially important in considering dose-escalation schemes that invariably test the limits of normal tissue tolerance within or in proximity to the PW. Various target volumes (GW, CW, PW, etc.) should be carefully designed considering the inherent limitations or uncertainties at each step of the process. The final PW should be based not only on the given imaging data and other diagnostic studies but also the clinical experience that has been obtained in the management of that disease. Tightening of field margins around image-based GW, with little attention to occult disease, patient motion, or technical limitations of dose delivery, is a misuse of 3-D CRT concept that must be avoided at all cost [59]. Conformal radiotherapy conforms or shapes the prescription dose volume to the planning target volume (PTV) as shown in figure 2.1 while at the same time keeping the dose to specified organs at risk at doses below their tolerance dose. The conformal radiotherapy chain is based on 3D target localization, 3-D treatment planning, and 3-D dose delivery techniques [1].

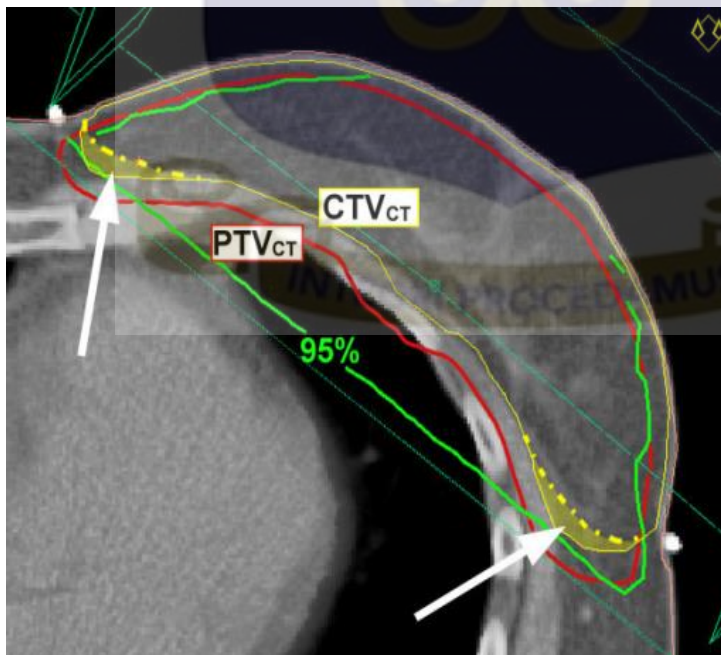


Figure 2. 1: 3D conformal EBRT Target Volume Construction

2.1.2. Treatment Planning Systems

Treatment planning system is typically comprised of: a means for inputting patient data (such as a digitizer or an interface to a computed tomography (CT) scanner); a computer which performs the dose calculation; and finally, a means of outputting the results of the calculations, the image, and the geometrical data, which are all elements used as the basis for the calculations. They are used in external beam radiotherapy to generate beam shapes and dose distributions with the intent to maximize tumour control and minimize normal tissue complications. Patient anatomy and tumour targets can be represented as 3-D models [41].

The main distinction between treatment planning of 3-D CRT and that of conventional radiation therapy is that the former requires the availability of 3-D anatomic information and a treatment-planning system that allows optimization of dose distribution in accordance with the clinical objectives. The anatomic information is usually obtained in the form of closely spaced transverse images, which can be processed to reconstruct anatomy in any plane, or in three dimensions. Depending on the imaging modality, visible tumour, critical structures, and other relevant landmarks are outlined slice-by-slice by the planner [59]. The radiation oncologist draws the target volumes in each slice with appropriate margins to include visible tumour, the suspected tumour spread, and patient motion uncertainties. This process of delineating targets and relevant anatomic structures is called segmentation. The next step is to follow the 3-D treatment-planning software to design fields and beam arrangements. One of the most useful features of these systems is the computer graphics, which allow beam-eye-view (BEV) visualization of the delineated targets and other structures. The term BEV denotes display of the segmented target and normal structures in a plane perpendicular to the central axis of the beam, as if being viewed from the vantage point of the radiation

source. Using the BEV option, field margins (distance between field edge and the PW outline) are set to cover the PW dosimetrically within a sufficiently high isodose level (e.g., >95% of the prescribed dose) [59]. Ordinarily a field margin of approximately 2 cm is considered sufficient to achieve this, but it may need further adjustments depending on the given beam profile and the presence of critical structures in the vicinity of the PW. Nonetheless, it is important to remember that each beam has a physical penumbra (e.g., region between 90% and 20% isodose level) where the dose varies rapidly and that the dose at the field edge is approximately 50% of the dose at the centre of the field [59]. For a uniform and adequate irradiation of the PW, the field penumbra should lie sufficiently outside the PW to offset any uncertainties in PW. Optimization of a treatment plan requires not only the design of optimal field apertures, but also appropriate beam directions, number of fields, beam weights, and intensity modifiers (e.g., wedges, compensators, dynamic multileaf collimators, etc.) In a forward planning system, these parameters are selected iteratively or on a trial-and-error basis and therefore, for a complex case, the whole process can become very labour intensive if a high degree of optimization is desired. In practice, however, most planners start with a standard technique and optimize it for the given patient using 3-D treatment-planning tools such as BEV, 3-D dose displays, non-coplanar beam options, intensity modulation, and dose-volume histograms. The time required to plan a 3-D CRT treatment depends on the complexity of a given case, experience of the treatment-planning team, and the speed of the treatment-planning system. The final product, the treatment plan, is as good as its individual components, namely, the quality of input patient data, image segmentation, image registration, field apertures, dose computation, plan evaluation, and plan optimization [59].

2.1.3 Treatment Techniques of Radiotherapy

For whole breast radiotherapy, the treatment target of BCT cases includes the remaining breast tissue and conditionally the regional lymphatics, namely supraclavicular, axillary and internal mammary lymph nodes. The location of breast target volume is superficial to the pectoralis major muscle above the anterior thoracic wall. The breast tissue usually extends from the midline to near the mid axillary line and cranial-caudally from the second or third anterior rib to the inframammary fold [60]. In the routine practice, a treatment regimen with dose of 45 – 50 Gy in 25 – 28 fractions of 1.8 – 2.0 Gy over 5 weeks is given to patients using tangential opposing field arrangement. An electron boost is also recommended to patients receiving lumpectomy with 10 – 16 Gy at 2 Gy per fraction to further decrease the local failure rate [61]. The main challenges of breast irradiation are offering adequate and homogeneous dose distribution to the target regions while preventing the surrounding organs at risk (OAR) from exceeding the tolerance. Radiation to the normal tissues, such as lung, heart and mediastinal tissues, should be minimized, whereas cosmetic problem owing to overdose should be avoided. Besides, the treatment planning is complex since it should take into considerations of some issues, such as wide and non-solid target, complex and concave target shape with regional lymph node irradiation and OAR avoidance, sufficient skin dose requirement, and moving target with respiratory motion [60]. According to the International Commission on Radiation Units and Measurements (ICRU) Report No. 50, the uniformity of the target dose is recommended to be between +7% and -5% of the prescribed dose within the target volume [2]. Regarding these criteria, patients' condition, clinical, radiologic and pathologic examination data are considered individually for the planning procedure. Conventionally, a two-dimensional (2D) planning system and a 2D contour with 1 to 3 transverse contours through the breast

and the lung are used to perform the treatment planning of tangential breast radiotherapy. Manual interactive optimization of the wedge compensator angle is carried out to compensate for the varying breast contour [62]. With the incorporation of computed tomography (CT) as well as the advances in computer engineering and software design, targets and avoidance structures can be easily defined on axial images, enabling the introduction of complex and accurate radiotherapy treatment techniques. The dose at each point within the entire three-dimensional (3D) irradiated volume can be calculated precisely by the use of modern dose calculation algorithms. Together with the new computer-controlled treatment delivery systems with multileaf collimator (MLC) and sophisticated 3D planning tools, such as advanced imaging technology for tumour and normal organ segmentation, the beam's-eye view technique, 3D dose-distribution displays, and structure-specific dose volume histograms (DVHs), a uniform dose distribution conformed to the target volume can be generated by three-dimensional conformal radiotherapy (3DCRT) technique [63]. Owing to consideration of the continuous change in the shape of the breast in multiple planes and the influence of the low-density lung tissues, improved dose homogeneity within the target volume can hence be achieved compared to the conventional technique [64]. Intensity modulated radiotherapy (IMRT) is an advanced form of 3DCRT. It employs specialized computer driven technology to generate improved dose distributions that conform to target regions with high precision. There are two approaches for IMRT planning, namely forward and inverse planning. The former starts with a preliminary selection of a set of beam parameters, such as directions, weighting, shapes and wedges, and initial dose distribution calculation. These parameters are subsequently adjusted until a satisfactory dose distribution is obtained. Additional MLC-shaped field segments, field-in-field, can be applied to optimize the plan manually. The multisegment-based forward planning

technique is useful for some relatively simple cases, but a more sophisticated inverse planning technique is necessary for more complicated cases. Inverse planning employs computer-aided optimization to generate treatment fields with varying intensities across the beam profiles. Intensity modulation can be achieved either by dynamic MLC or multi-segment static, or step-and-shoot MLC. Contrast to forward planning, it is based on dose objectives to the target and surrounding OAR defined by user, and an iterative computer optimization program to produce a solution plan that fulfils the specified criteria as closely as possible. The resultant dose distribution, usually consisting of multiple beams from various directions, can have high conformity with steep dose gradient [65, 66].

2.2 Volume Definition

Volume definition is essential for meaningful 3D treatment planning and for accurate dose reporting. The ICRU 50 and 62 [2, 3] reports define and describe several target and critical structure volumes that aid in the treatment planning process and that provide a basis for comparison of treatment outcomes. Gross tumour volume, clinical target volume, internal target volume, and planning target volume have been defined as principal volumes related to 3D treatment planning: Figure 2.2 shows how the different volumes are related to each other.

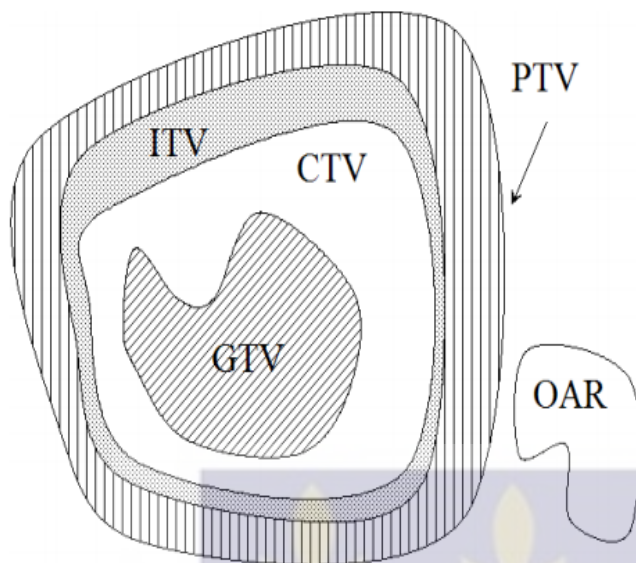


Figure 2. 2: Graphical representation of the volumes-of-interest, as defined by the ICRU 50 and 62 reports [2, 3]

2.2.1 Gross Tumour Volume (GTV)

The Gross Tumour Volume (GTV) is the gross palpable or visible/demonstrable extent and location of malignant growth” (ICRU 50) [2]. The GTV is usually based on information obtained from a combination of imaging modalities (CT, MRI, ultrasound, etc.), diagnostic modalities (pathology and histological reports, etc.) and clinical examination.

2.2.2 Clinical Target Volume (CTV)

The clinical target volume (CTV) is the tissue volume that contains a demonstrable GTV and/or sub-clinical microscopic malignant disease, which has to be eliminated. This volume thus has to be treated adequately in order to achieve the aim of therapy, cure or palliation” (ICRU 50) [2]. The CTV often includes the area directly surrounding

the GTV that may contain microscopic disease and other areas considered to be at risk and require treatment (e.g., positive lymph nodes). The CTV is an anatomical-clinical volume and is usually determined by the radiation oncologist, often after other relevant specialists such as pathologists or radiologists have been consulted. The CTV is usually stated as a fixed or variable margin around the GTV (e.g., $CTV = GTV + 1 \text{ cm margin}$), but in some cases it is the same as GTV (e.g., prostate boost to the gland only). There can be several non-contiguous CTVs that may require different total doses to achieve treatment goals.

2.2.3 Internal Target Volume (ITV)

Consists of the CTV plus an internal margin. The internal margin is designed to take into account the variations in the size and position of the CTV relative to the patient's reference frame (usually defined by the bony anatomy), i.e., variations due to organ motions such as breathing, bladder or rectal contents, etc. (ICRU 62) [3].

2.2.4 Planning Target Volume (PTV)

The planning target volume is a geometrical concept, and it is defined to select appropriate beam arrangements, taking into consideration the net effect of all possible geometrical variations, in order to ensure that the prescribed dose is actually absorbed in the CTV" (ICRU 50) [2]. The PTV includes the internal target margin (ICRU 62) [3] and an additional margin for set-up uncertainties, machine tolerances and intra-treatment variations. The PTV is linked to the reference frame of the treatment machine. It is often described as the CTV plus a fixed or variable margin (e.g., $PTV = CTV + 1 \text{ cm}$). Usually a single PTV is used to encompass one or several CTVs to be targeted by

a group of fields. The PTV depends on the precision of such tools as immobilization devices and lasers, but does not include a margin for dosimetric characteristics of the radiation beam (i.e., penumbral areas and build-up region) as these will require an additional margin during treatment planning and shielding design.

2.3 The Organs at Risk and Radiation Tolerance Doses

Organ at risk is an organ whose sensitivity to radiation is such that the dose received from a treatment plan may be significant compared to its tolerance, possibly requiring a change in the beam arrangement or a change in the dose. Specific attention should be paid to organs that, although not immediately adjacent to the CTV, have a very low tolerance dose (e.g., eye lens during nasopharyngeal or brain tumour treatments). Organs with a radiation tolerance that depends on the fractionation scheme should be outlined completely to prevent biasing during treatment plan evaluation [1]. Breast tissue/chest wall and regional lymphatics have close proximity to vital organs such as the lung, heart, and coronary arteries. Moreover, consideration should be given to the contralateral breast, contralateral lung, brachial plexus, oesophagus, thyroid, and spinal cord as well. The optimal delineation of organs at risk (OAR) carries substantial importance due to its influence on treatment planning evaluation. Inadequate delineation of OAR results in the misinterpretation of dose volume histograms (DVH) [70]. Therefore, differences in contouring are clinically and dosimetrically significant and a consensus is highly desirable.

2.3.1 Dose-Volume Constraints of contralateral breast

Several studies have indicated that there has been an increased risk of contralateral breast cancer, particularly in young women treated with RT [18, 28]. The dose to the contralateral breast is because of the medial tangent beam and the result of a collimator scatter, leakage, scatter from blocks and wedges, etc. Dosimetry studies have reported lower contralateral breast doses with IMRT as a result of not using the wedges [79]. The RTOG breast study protocol recommends keeping the Dmax of the contralateral breast <3–3.3 Gy [27]. Investigators had minimized the Dmax to <3.9 Gy and mean dose of 0.3 Gy for patients treated with multifield IMRT (9-field technique) [78].

2.4 Peripheral Dose

During radiation therapy, regardless of the treatment technique, the surrounding normal tissues outside the treated area inevitably receive some amounts of radiation dose. Such dose outside the geometric boundaries of the treatment fields is known as peripheral dose. There are three main sources of peripheral dose: (1) Leakage from the treatment gantry, (2) scattered radiation from the secondary collimators and beam modifiers such as wedges and MLC, and (3) internal scatter originating in the patient [67]. Mazonakis et al. examined that the peripheral dose from 6 MV photons ranged from 0.13% to 6.75% and that from 18 MV photon varied from 0.09% to 5.61% of the central-axis maximum dose [68]. They are affected by the collimator orientation, extent of irradiated area, and distance from the treatment field. The association between the low dose from ionizing radiation and the risk for secondary cancer has attracted new interest recently, especially for the long-term surviving patients [69]. Therefore, the peripheral dose delivered to some anatomical structures with high radiation sensitivity, such as the lung,

gonads and contralateral breast, is of great concern. Several factors were documented by Frass et al. [12] that can influence the peripheral dose, including radiation field technique, the wedge used, and shielding. Wedges are commonly used in many clinical situations to assist generating treatment plans with homogeneous dose distribution. Physical wedges, made of high-atomic number materials, of standard wedge angles 15°, 30°, 45° and 60° are available, while dynamic wedges use an upper independent jaw motion to create a wedge shaped distribution in some linear accelerators [71]. It is found that the employment of different types of wedges results in various peripheral doses [72].

2.5 Risk of Contralateral Breast Cancer

For breast cancer cases, more attention should be paid to the dose outside the radiation fields due to the fact that breast tissues and the regional lymphatics, locating at the chest region, have close proximity to many vital organs. The OAR include lung, heart, coronary arteries, contralateral lung, oesophagus, brachial plexus, thyroid and spinal cord. Apart from these structures, consideration should also be given to the contralateral breast [60]. Some studies showed that breast irradiation increased the rate of sarcomas, as well as lung cancers, especially in smokers [73]. Contralateral breast cancer (CBC) is the most common secondary malignancy in patients treated for first breast cancer, and it accounts for about 50% of all second primary cancers [15]. Their incidence rates at 5, 10, 15 and 20 years are 3.5%, 7.6%, 11.3% and 15.4% respectively, with the median diagnosis time being 8.2 years [16]. Some studies indicated that patients with age smaller than 45 years at the time of the primary breast cancer diagnosis, women of black race, tumour histology of lobular carcinoma and medullary carcinoma, positive family history, as well as BRCA 1 and BRCA 2 gene mutation carriers are associated

with increased risk of the disease [15, 16]. The induction of second malignancy by radiation is believed to be a stochastic process with no threshold dose and has a dose-dependent relationship [76]. Regarding the potential hazard, the Radiation Therapy Oncology Group (RTOG) breast study protocol recommended that the dose maximum (Dmax) of the contralateral breast should be kept under 3 – 3.3 Gy [60].

2.6 Radiation Dosimeters

A radiation dosimeter is a device, instrument or system that measures or evaluates, either directly or indirectly, the quantities exposure, kerma, absorbed dose or equivalent dose, or their time derivatives (rates), or related quantities of ionizing radiation. A dosimeter along with its reader is referred to as a dosimetry system. Measurement of a dosimetric quantity is the process of finding the value of the quantity experimentally using dosimetry systems. The result of a measurement is the value of a dosimetric quantity expressed as the product of a numerical value and an appropriate unit. To function as a radiation dosimeter, the dosimeter must possess at least one physical property that is a function of the measured dosimetric quantity and that can be used for radiation dosimetry with proper calibration. In order to be useful, radiation dosimeters must exhibit several desirable characteristics. In this context, the desirable dosimeter properties will be characterized by accuracy and precision, linearity, dose or dose rate dependence, energy response, directional dependence and spatial resolution. Obviously, not all dosimeters can satisfy all characteristics. The choice of a radiation dosimeter and its reader must therefore be made judiciously, taking into account the requirements of the measurement situation [1].

2.6.1 Radiochromic Films

The focus of any dosimetry system is always the dosimeter. A dosimeter is defined as a device that undergoes a measurable change when irradiated [56]. Radiation dosimetry for industrial and medical purposes has advanced over the last few decades with the introduction of various new detectors. Many different detectors have their specific areas of applications depending on the qualities for radiation dosimetry they exhibit [36]. In physics an ideal dosimeter should be able to measure absorbed dose i.e. energy absorbed per unit mass. With the current development in the accuracy and precision of film manufacturing, in addition to the sharpness and ease of use, the widespread use of radiochromic dosimeters in medical and nonmedical applications has increased [32]. Over the past several years the dosimetric properties of radiochromic dosimeters have been assessed by many investigators and extensive literature on various aspects of radiochromic dosimetry has been published. Radiochromic media for dosimetry can be found in various forms including liquid solutions, gels, waveguides and films. Radiochromic film responds to ultraviolet light or ionizing radiation by turning blue, with two nominal absorption bands ($\lambda_{max} = 670$ and 610 nm) which depend on the absorbed dose, temperature during irradiation, as well as post irradiation reading time [32]. According to literature, the radiation induced colour change of the film is formed directly without thermal, optical, or chemical change and the original blue image is stable at temperatures up to about 60°C above which the colour of the image changes sharply from blue to red. The image formation in radiochromic products occurs as a dye forming or a polymerisation process, in which energy is transferred from an energetic photon or particle to the receptive part of the leuco-dye or colourless photo monomer molecule, introducing a colour formation through chemical changes. This film has very little dependence on relative humidity

during irradiation, but there is a marked temperature dependence, the degree of which varies with radiation dose and temperature level [36]. Their dosimetric ranges also cover a wide range from doses as low as 0.1 up to 106 Gy. Radiochromic films come in various types such as Gafchromic films which have been identified by the catalogue number of a supplier, Nuclear Associates.

2.6.1.1 Configuration and Structure of Gafchromic EBT2

Gafchromic film (International Specialty Products (ISP), Wayne, NJ) [46] is a type of self-developing radiochromic film that was introduced in 2004 and it is becoming well-known as a suitable dosimeter in radiology [33] and radiation oncology applications. It is self-processing and does not require handling in a dark room like the traditional films. Gafchromic film is versatile; it can be easily cut, immersed in water and handled in room light. Gafchromic EBT2 film is a specific brand and model of radiochromic film produced by International Specialty Products (ISP) Corporation (Wayne, NJ). Gafchromic EBT2 is prepared by combining a clear, polyester over-laminate with the active film coating. The substrate of the active film is clear 700 gauge (175 micron) polyester. The substrate is coated with an active layer film, nominally 28 microns thick. The over-laminate, 200 gauge (50 micron) polyester with approximately 25 microns of pressure-sensitive adhesive, is fused to the coated side of the active film [45]. The configuration of EBT2 is shown in figure 2.3. The structure of EBT2 film is non-symmetric. When EBT2 is scanned it could be oriented with either the polyester laminate or the polyester base facing the light source.

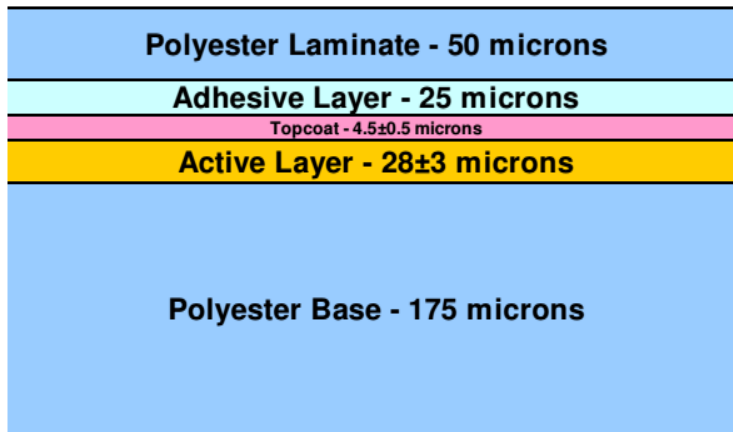


Figure 2. 3: Configuration of GAFCHROMIC EBT2 Film [45]

The active layer is protected by the over-laminate from mechanical damage as well as from the effects of water and other liquids. Unlike the previous EBT film, the new version can be immersed in water for short periods and the water will only penetrate 1-2 mm. The parts affected by the water are easy to see because they turn opaque. Except for these areas the performance of the remaining film is unchanged. The active layer contains the same radiation-sensitive component used in the original EBT version of radiochromic film. However, the binder in the active layer has been changed from a natural polymer, gelatin, to a synthetic polymer [45]. The synthetic polymer provides a better control of the atomic composition of the active layer. The synthetic polymer also makes it possible to apply the active material as a single layer coating. In the early part of 2010 the use of a topcoat layer in EBT2 was eliminated [45]. This was done by incorporating antioxidants and stabilizers directly in the active layer. A prominent feature of EBT2 is its yellow colour. The yellow colour arises from the presence of a yellow dye integrated into the active layer. The dye referred to as a marker dye serves the purpose of establishing a baseline against which the response of the film can be measured. As a result, it is now possible to use an RGB scanner to calibrate the film response in all three colour channels and with special software, Film QA Pro 2010, to

divide a film image into dose-dependent and dose independent parts [45]. By doing this many film and scanner artefacts can be eliminated thereby improving the integrity of the dose-dependent image and the accuracy of the dosimetry.

2.6.1.2 Gafchromic EBT2 Dosimetry Film Characterization and Measurement

Film dosimetry is a powerful tool for radiotherapy treatment verification and quality assurance. Over the years there have been significant improvements in the sensitivity and uniformity as two-dimensional detectors [38]. Recently, film dosimetry has gained increased popularity in brachytherapy, diagnostic radiology, and radiobiological experiments. Two-dimensional arrays of diodes or ion chambers can produce results in real time, but film has the advantage of higher spatial resolution (25 μm). The spatial resolution of dosimeters is limited by the finite nature of dosimeter size and collecting volume. In the microscopic scale, the spatial resolution is limited by the stochastic nature of energy deposition in matter. Several studies have researched into the energy response of different film dosimeters over a wide range of photon energies, and Gafchromic EBT2 film has been demonstrated to have minimal energy dependence in the megavoltage energy range a necessary attribute when working with a ^{192}Ir source. Yet this film is generally insensitive to ambient room lighting. There are data to indicate variation with energy for kilovoltage x-rays as shown in figure 2.4 [31]. The high sensitivity radiochromic film has been designed for the measurement of absorbed dose of high-energy photons used in IMRT. The film has been designed to measure doses up to at least 30 Gy when used with an RGB colour scanner. At doses above 10Gy the response in the red colour channel approaches saturation, so in the case of single channel dosimetry it is preferable to change to the green colour channel for these measurements. While it may be possible to extend measurement to 50 Gy without

utilizing the marker dye feature [45]. EBT2 Gafchromic film was designed for use in the energy range 50 kiloelectron volt (keV) into megavolt (MV) and with sensitivity down to 1 cGy. The upper dose limit is 10 Gy if measuring in the red channel [46].

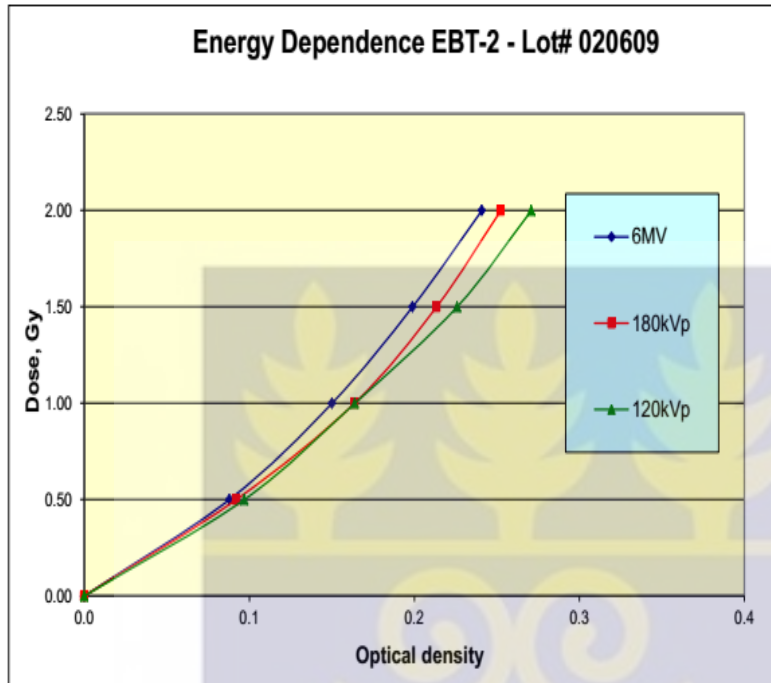


Figure 2. 4: Energy Dependence of GAFCHROMIC EBT2 Dosimetry Film [46]

It is near tissue equivalent ($Z_{eff} = 6.84$), has high spatial resolution and exhibits weak energy dependence. The film contains an active layer with particles that polymerise and turn blue when exposed to ionising radiation. A yellow marker dye is incorporated into the active layer of the film which protects the active component from exposure to visible and UV light. Additionally, the dye can be used to improve dose accuracy, if measured on a colour scanner, by applying corrections for the non-uniformity in the film thickness. The film is digitised on a flatbed scanner and the absorbed dose is obtained by analysing the optical density of the film with respect to dose. The absorbed dose to the film is calculated by accurately quantifying the amount of light transmitted through the film after radiation exposure. The intensity of light transmitted through the

film is measured and converted to an optical density (OD). Using this value, a relation between the absorbed dose and film opacity is established. This method has been widely used in many other studies to great effect [40]. Optical Density is defined as the logarithm of the ratio between the intensity of incident light collected with the film absent (I_0) and the intensity of the transmitted light (I) through the film given as

$$OD = \log_{10} \frac{I_0}{I} \quad 2.1$$

Net optical density (net OD) is another value of importance calculated by subtraction of a blank or unexposed film from an exposed film used in a measurement. A Hurter–Driffield curve (H-D curve) or sensitometric curve is then derived. The H-D curve is a plot created to show the net OD as a function of radiation exposure as shown in figure 2.5.

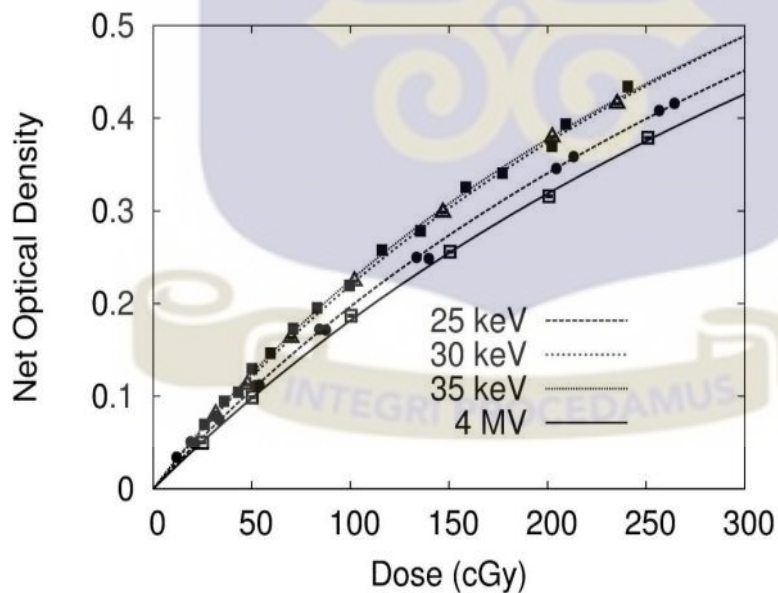


Figure 2. 5: Net optical density versus dose for EBT2 film. The film was calibrated at 25 keV (circles), 30 keV (triangles), 35 keV (filled squares) and 4 MV (hollow squares) [35].

Literature reports that the highest uncertainty in the dose measurements is due to the scanning technique used, nevertheless, this can be reduced significantly if a laborious scanning protocol is adhered to [53]. The film continues to darken over time after irradiation and the darkening behaviour is dose dependent [50]. In order to overcome the problem of energy dependence, it is recommended that the post irradiation scan time of the calibration and measurement films be kept consistent. The work of Devic et al. [39], showed that a 1% dose error can be achieved if a scanning window of ± 2 h is used for a 24 h post irradiation scan time. The uniformity of the scanner factors into the film response; differences of up to 5.5% have been reported depending on the position of the film on the scanner bed [53]. The alignment of the polyester substrate layer (i.e., facing towards or away from the glass) has little effect on the optical density for doses higher than 1 Gy (less than 1%) [30]. These authors suggest an alternative scanning in the portrait orientation produces variations of up to 9%.

2.6.1.3 Scanning of Gafchromic films

EBT2 film can be read with a film scanner or digitizer. The best response is obtained if the film is scanned in transmission, and the spectral response of the scanner is matched to the absorbance of the film [45]. An example of this is the Vidar DosimetryPRO Advantage (Red) scanner with the red LED light source. The LEDs in this scanner have maximum emission at a wavelength close to 630 nm, and thus well matched to the spectral maximum in EBT2 film [45]. Other examples are rgb colour scanners, e.g. Epson, Microtek, Canon, HP designed to scan colour films in the red, green, and blue bands of the visible spectrum. Once an rgb scan has been obtained the user can extract the information from the red colour channel where the active component in EBT2 film

produces its maximum response. With some scanners, e.g. Epson Expression 10000XL Graphic Arts, it is necessary to purchase a transparency adapter to obtain transmissions scans. HeNe laser scanners (Lumisys, Array, Molecular Dynamics) can provide the highest response with EBT2 film because the laser has a wavelength of about 633 nm, nearly at peak absorbance. However, the coherent light of the laser scanners can produce artefacts caused by the interaction of polarized light with the film [45].

GAFCHROMIC EBT2 dosimetry film contains a yellow marker dye. When an rgb colour scanner is used to digitize the EBT2 film, the marker dye makes it possible to obtain a response signal that is proportional to thickness, and thereby to compensate for small non-uniformities in the film. Because the dye is yellow, it produces a strong signal in the blue colour channel, but no signal in the red colour channel. Since the marker dye has no response in the red channel it does not interfere with the signal produced by exposure of the active component [45]. However, the active component does produce a small response in the blue colour channel, and this must be accounted for before the response from the marker dye can be used to compensate for thickness differences [45]. The use of the marker dye takes advantage of an inherent feature of an rgb scanner, that is, its ability to acquire scan measurement simultaneously in three colour channels. Not only does this save the necessity of separate scans for each channel, but it also ensures that the response values from all the colour channels are in close spatial registration [45]

2.6.1.4 Film Calibration and Sensitivity

Calibration of the film response is the first requirement of a film dosimetry protocol. It is of the utmost importance in establishing the accuracy and repeatability of the overall

dosimetry measurement and evaluation process. Radiochromic film has been shown to be suitable for dose measurements in surface and near surface regions due to its energy independence, tissue equivalency, and high sensitivity [55]. The present study employed radiochromic Gafchromic EBT2 film (hereafter called EBT2 film) as a principal dosimeter to measure contralateral breast dose. Thuo, [57] calibrated the Gafchromic EBT2 by using Monte Carlo Non-Particle (MCNP) output (MeV/decay) converted to radiation dose per photon emitted. The author exposed the films for some selected periods of time to result in a given dose. The exposed films were then scanned and the corresponding intensity read out from analysis software along with a calibrated converted pixel values to dose. According to the author, each of the data point represents and average optical density over three scans. Optical density is proportional to radiation dose absorbed in the film. Pixels of the scanned digital image contain information on intensity of the light transmitted through the film to the light-sensitive elements of the scanner. The calibration curve obtained by this author is given in figure 2.6

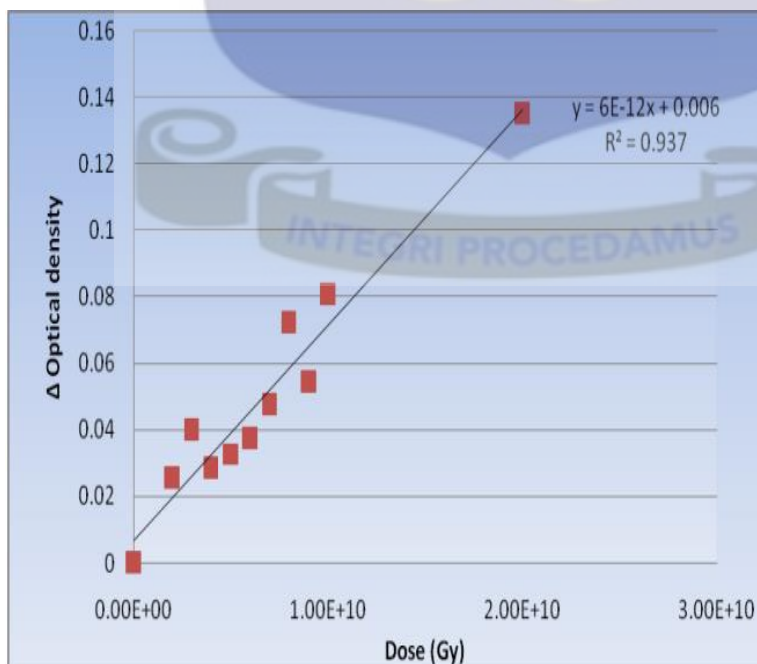


Figure 2. 6: GafChromic EBT2 film response curve over 10cm² [57]

The calibration curve can provide information for conversion of film response to dose and vice versa. The relationship between dose and film response can also be tabulated. The change in film response per unit absorbed dose can be represented by a single number for a net optical density up to 1.0. This number, defined here as film average sensitivity, is the average change in response (i.e., readout) per unit absorbed dose calculated over the lower, most linear portion of the calibration curve. This number depends on one or more of the following:

- (1) the wavelength used for readout,
- (2) the particular densitometer used for readout,
- (3) film batch,
- (4) the delay between irradiation and readout,
- (5) beam quality of the calibration source, and
- (6) other factors (such as temperature and humidity) previously discussed.

2.7. Multileaf Collimators (MLC)

As early as 1959 a patent for a multileaf collimator (MLC) to be attached to a therapy machine was published [42]. This comprised sets of movable blocks (or leaves) orthogonally disposed which could collimate an irregular beam shape. Most modern MLCs have leaves which move in only one direction and the principle of orthogonal pairs does not seem to have been developed further. The leaves were moved manually until they gripped a template of the desired shape. This principle has been continued with modern manual MLCs. Historically MLCs have been used since the early part of the century to collimate diagnostic beams [49]. However the concept of the modern MLC for therapy machines was embodied in the patent by Brahme (1985/7) [43] which described all the required features of such a device. These features include double-

focusing, automatic leaf setting, stepped leaf edges to reduce interleaf penetration, narrow leaves and a method for verifying the field shape. The ideas in this patent were adopted in the Scanditronix commercial product. Essentially each pair of leaves defines a strip of radiation which is matched to the projected area of the target in a thin slice of the patient. Much of this earlier works in radiotherapy was purely theoretical, with no knowledge of how the optimised, modulated beams would be physically produced. The use of various beam modifiers, such as metal compensators, were proposed but this was impractical due to the specificity of each patient, field and field segment [34]. This was overcome as MLCs became commercially available in the early 1990s. Consisting of multiple individually driven tungsten leaves, MLCs were originally designed for beam shaping in 3DCRT, but would soon become invaluable in the delivery of IMRT treatments. The first publication outlining a feasible method for delivering arbitrary intensity profiles using an MLC that moved dynamically, in a unidirectional sweep throughout treatment, was published in 1992 [37]. Here, relatively large dynamic apertures are used with the field open to areas of high intensity for a larger fraction of time than areas of low intensity, hence producing a profile with varying modulation. MLCs that move dynamically throughout treatment are an essential component of IMRT treatment delivery [34].

This model was subsequently improved to include the finite acceleration and velocity of individual leaves, leaf transmission and penumbra effects, to form the basis for modern sliding window IMRT delivery [34]. A separate delivery method was developed independently and simultaneously, whereby each intensity profile is built up using a succession of discrete field segments each delivering a fraction of the total field fluence. This work was the basis for the modern step-and-shoot IMRT.

Each intensity-modulated delivery technique has advantages and disadvantages, but the driving force for step-and-shoot being the fact that MLC movements are made while the beam is off and therefore the probability for an error in treatment may be reduced [34]. The introduction of multileaf collimators into radiation oncology has provided many advantages, while at the same time introducing new challenges. Multileaf collimators, when used as a replacement for conventional blocks, reduce the time required by eliminating the block production process, as well as reducing the time required for the radiation therapist to set up between sequential fields [47].

2.8. Wedges

Wedges are beam modifying devices to homogenize the dose distribution. They slant the dose distribution in a defined depth towards a desired angle over the beam. This is achieved by a progressive decrease in intensity across the beam (from the thin edge to the thick edge of the filter). This results in an isodose distribution with a planned asymmetry. The tilt degree depends on the slope of the wedge filter. Wedges are generally used for relatively superficial tumours [54].

The following wedge types exist:

- Static wedge (manual): Fixed design
- Motorized wedge (also known as dynamic wedge): Wedge (with a fixed design) is moved into the beam field for part of the time to create the wedge beam profile
- Virtual wedge (also known as dynamic enhanced wedge): Are created by computer controlled movement of one of the collimator jaws while

concurrently adjusting the dose rate and the jaw's moving speed during the irradiation

Physical wedges are angled pieces of lead or steel that are placed in the beam to produce a gradient in radiation intensity. Manual intervention is required to place the physical wedges on the treatment unit's collimator assembly. A motorized wedge is a similar device, a physical wedge integrated into the head of the unit and controlled remotely. A dynamic wedge produces the same wedged intensity gradient by having one jaw close gradually while the beam is on [52]. A typical isodose distribution for a wedged beam is shown in figure 8.

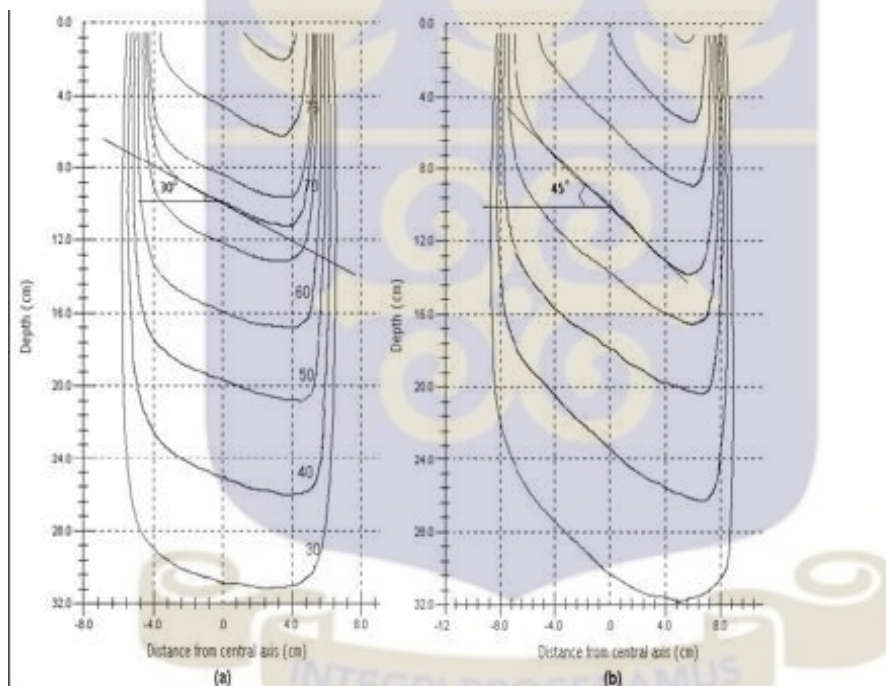


Figure 2. 7: Isodose curves for a wedged 6 MV photon beam. The isodoses have been normalized to Z_{max} with the wedge in place [54].

- The thick end of the wedge is called the heel; the dose is lowest underneath this end. The other end is called the toe.

- Wedge angle is defined as the angle between the 50% isodose line and the perpendicular to the beam central axis. Wedge angles in the range from 10° to 60° are commonly available [54].

Wedges have two main uses in radiotherapy:

They can be used to compensate for a sloping surface, as for example, in nasopharyngeal treatments where wedges are used to compensate for decreased thickness anteriorly, as shown in figure 9.

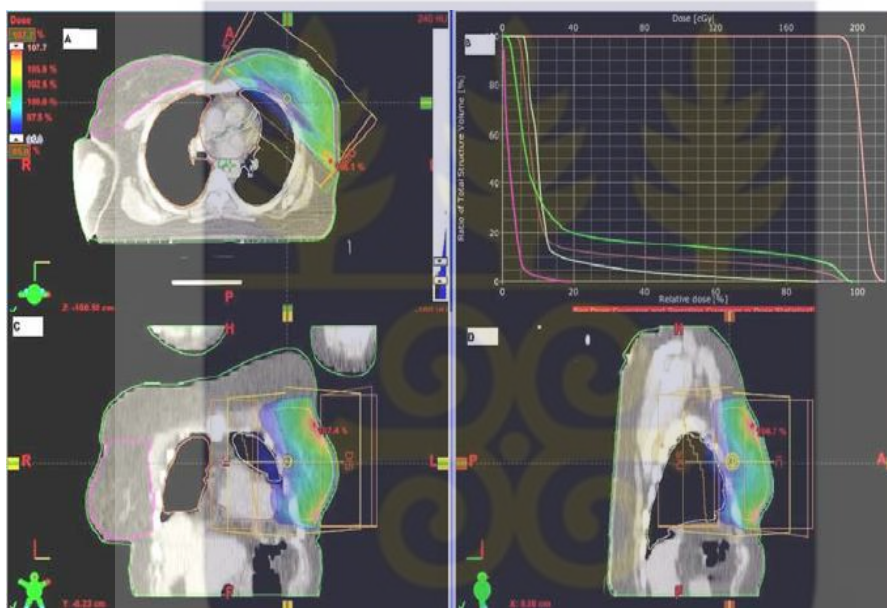


Figure 2. 8: Conformal radiotherapy with wedges (CRT-W) technique: a) Transverse slice of CRT-W. b) Dose volume histogram (DVH): pink colour: PTV, green colour: ipsilateral lung, brown colour: heart, light green colour: LAD and magenta colour: contralateral breast. c) Frontal slice of CRT-W. d) Sagittal slice of CRT-W. [80].

The optimal wedge angle (assuming a flat patient surface) may be estimated from: $90^\circ - 1/2$ (hinge angle). The wedge factor is therefore defined as the ratio of dose at a specified depth (usually z_{\max}) on the central axis with the wedge in the beam to the dose under the same conditions without the wedge. This factor is used in monitor unit

calculations to compensate for the reduction in beam transmission produced by the wedge. The wedge factor depends on depth and field size [52].

Physical wedges are used to modulate the intensity of radiation. Principally, they represent absorbent blocks made from metallic material and they are placed into the path of X-ray beam at the output of an accelerator. They modify a dose distribution because of their shape (thin at one side and thick at the other side), so a dose gradient across the entire field is formed.

Wedge angle describes how big the gradient is. Several definitions of this term exist. According to ICRU (International Commission on Radiation Units and Measurements) the wedge angle is defined as the angle through which an isodose is tilted at the central axis of the beam at a specified depth (usually 10 cm) (Cherry and Duxbury, 1998) (Fig 2) [77]. Physical wedges are made to provide four specific wedge angles: 15°, 30°, 45° and 60°.

Enhanced dynamic wedges substitute the physical wedges. This technique achieves wedge-shaped dose distributions by computer-controlled movement of one of the collimator jaws (Fig. 3) under simultaneous adjustment of dose rate and speed of the moving jaw during the irradiation [80]

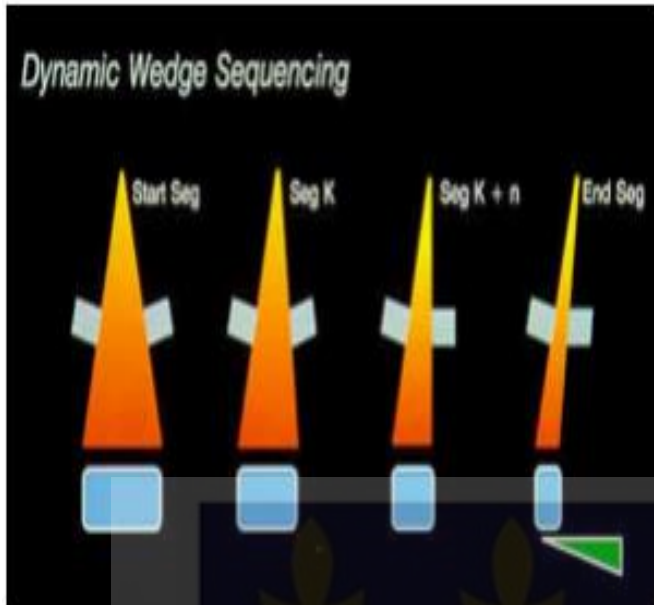


Figure 2. 9: Principle of the EDW [80]

Dynamic wedges have several advantages over the conventional physical ones: they eliminate the physical wedges; they can generate any arbitrary wedge angle; they reduce a treatment time; they reduce a dose that is outside the treatment plan and they provide better dose distributions of a straight isodose line without beam hardening. The main disadvantage of the EDW is a necessity of a systematic control and a verification of reliability and stability of the EDW [80]



CHAPTER THREE

MATERIALS AND METHOD

3.0 Introduction

The methodologies adopted to estimate doses to the contralateral breast using calibrated Gafchromic EBT2 films are presented in this chapter. Calibration of Gafchromic EBT2 films for estimating contralateral breast dose with anthropomorphic female Rando phantom together with dose measurements are outlined. The study was carried-out at the Radiotherapy unit of Sweden Ghana Medical Centre.

3.1 Materials

The materials used in this study were Elekta Synergy 11 Platform Linear Accelerator unit, Gafchromic EBT2 films, anthropomorphic female Rando phantom, plastic water (PPMA) phantom, ScanMaker 9800XL plus, Oncentra® Master Plan version 4.3 Treatment Planning System (TPS)

3.1.1 Elekta Linear Accelerator unit

The Elekta Synergy 11 prototype linear accelerator (Elekta AB, Stockholm, Sweden) with a standard 80 leaf MLC head was used for the measurements. The linac is fitted with a motorized wedge and an iBEAM evo carbon fibre couchtop. The LINAC has dual energy photon beams of 6 MV and 15 MV and electron beams of 6, 10 and 15 MV. With the help of the multileaf collimator (MLC), the treatment beams are collimated, filtered and monitored within the treatment head of the LINAC in order to produce a clinically useful radiation beam which delivers a uniform dose distribution

at a specified depth in water. LINACs are calibrated by medical physicists to deliver a specific radiation dose at the isocentre with a high degree of accuracy. It is around this isocentre that all treatment plans are designed. The machine output is measured in monitor units (MU) in which individual machines are calibrated to deliver a specific absorbed dose per MU (usually 1Gy/MU). The Figure below is the linear accelerator (LINAC) used for treating cancer patients in Sweden Ghana Medical Centre.



Plate 3. 1: Elekta Linear Accelerator unit

3.1.2 Gafchromic film (EBT2)

Gafchromic film EBT2 with lot number #A08221302 produced by the International Specialty Product with sheet size of 14''×17'' was used in this work. The EBT2 dosimetry film is designed to measure absorbed dose in both high-energy photon beams

and in regions of steep dose gradients due to their high spatial resolution. The films were designed to measure doses up to at least 30 Gy when used with an RGB colour scanner. At doses above 10 Gy, the response in the red colour channel approaches saturation, so in the case of single channel dosimetry, it is preferable to change to the green colour channel for these measurements. The EBT2 film has a threshold dose of ~ 1 cGy but also depends on the reading out system. The Gafchromic dosimetry technique is nearly energy independent from about 50 keV into the MV. In addition, the technique is self-developing, relative ease of use and ease of analysing data [22]. Each sheet has a size of $8\text{ cm} \times 10\text{ cm}$, which was cut to $2\text{ cm} \times 3\text{ cm}$ for calibration as shown in figure. 3.2.

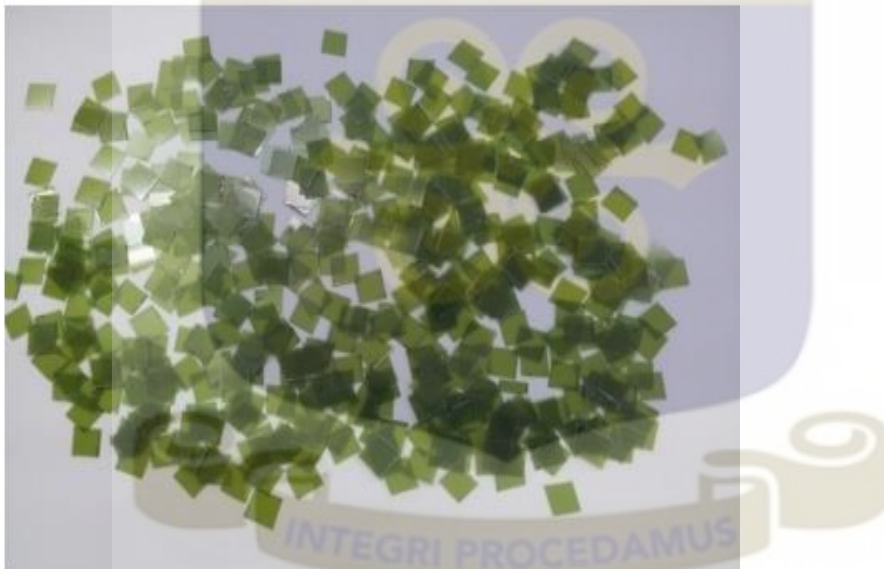


Plate 3. 2: $1\text{ cm} \times 1.5\text{ cm}$ pieces of Gafchromic EBT2 film.

3.1.3 Rando Alderson Phantom

An anthropomorphic female Rando phantom was used as the subject in this study (Figure 3.3). It is tissue-equivalent and simulates the physical characteristics of human body outline and body composition. Patient dose measurements are thus frequently

carried out in a Rando phantom. It is straightforward to make dose measurements at any given point inside the phantom. [23]. Hence the data obtained from the anthropomorphic phantom can be used to simulate the real situations.



Plate 3. 3: An anthropomorphic female Rando phantom

3.1.4 Mini Water Phantom

A plastic water phantom of dimensions; 30 cm x 30 cm was used for the calibration of the Gafchromic films. The EBT2 films were placed perpendicular to the beam central axis at a depth of 5 cm in the plastic water phantom. It is made of Perspex (PMMA) and has a field size of 10 cm x 10 cm inscribed on one of its surfaces. At one of the sides is a hole provided by the manufacturer to accommodate 0.6 cc farmer type ionization chamber. On one of the surfaces is an opening used for filling the phantom with water for the beam output measurement. Figure 3.4 is a diagram of the mini water phantom used in this research showing reference field size condition.

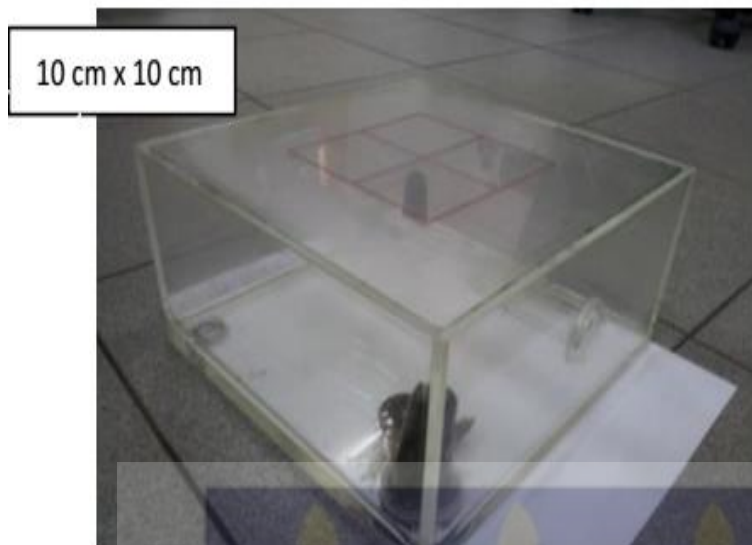


Plate 3. 4: Mini water phantom

3.1.5 ScanMaker 9800XL Plus

The EBT2 films were scanned using ScanMaker 9800XL plus (Microtek Inc. Santa Fe Spring, CA). The ScanMaker 9800XL Plus contains a larger-format (12" x 16") TMA (Transparent Media Adapter) that allows you to scan various transparent films easily.

The ScanMaker 9800XL Plus has a CCD with resolution that reaches up to 1600 x 3200 pixels per inch. With the built-in 48-bit ADC (Analog to Digital Converter), the ScanMaker 9800XL Plus can convert originals to digital data with high fidelity format. It is capable of delivering full 48-bit depth colour for richer and smoother tonal values; also, an optical range of 3.6 Dmax allows users to capture details in highlight and shadow areas, as well as accurately represents gradation and natural colour from originals without sacrificing details of the image.

3.2 Experimental Method

3.2.1 Calibration and irradiation procedures of Gafchromic EBT2 films

Gafchromic film EBT2 with lot number #08221302 was used in this work. The films were handled with care to avoid fingerprints and were prepared on a clean surface. The orientation of the film was marked as soon as it was taken out from the box to minimize inaccuracies in measured optical density and thus measured dose due to orientation effects.

Film set A were exposed in a phantom composed of $30 \times 30 \text{ cm}^2$ sheets of solid water (PTW, Freiburg, Germany) with 10 cm of the build-up material above and below the film. The field size was set to $10 \times 10 \text{ cm}^2$ and source-to-surface distance (SSD) of 100 cm. A total of 14 pieces of cut films ($2 \times 3 \text{ cm}^2$) were irradiated with the 6 MV radiation beam from the Elekta Synergy linear accelerator for a specified treatment time determined by the Ocentra Master plan TPS for a similar geometry and setup. The films were given uniform radiation doses of 0.0 cGy, 25cGy, 50 cGy, 75 cGy, 100 cGy, 125 cGy, 150 cGy, 175 cGy, 200 cGy, 225 cGy, 250 cGy, 275 cGy, 300 cGy and 325 cGy. The film dose response was calibrated for 6 MV photon beam in accordance with recommendations found in the TG-55 document [19].

The films were placed around the central axis of the beam at the depth of dose maximum ($d_{\text{max}} = 1.5 \text{ cm}$). The absorbed dose from the Linac was measured using a calibrated ionization chamber. A number of tissue-equivalent materials (15 cm), placed below film pieces, were used to provide full backscatter.

The EBT2 films were scanned using a Microtek ScanMaker 9800XL (Microtek Inc. Santa Fe Spring, CA) 24 hours after irradiation. This was to allow for maximum post irradiation coloration [20]. Scanning of the films was done in transmission mode.

Scanning orientation was kept consistent for all films. This is because EBT2 film exhibits a different response in portrait orientation compared to the response in landscape orientation of 7%–9% [30]. The data were analysed using ImageJ v1.45s. (National Institute of Health, Bethesda, MD) by splitting the film image data into red, green, and blue colour channels. For each scanned image and colour channel, a region of interest (ROI) of $3.4 \times 5.0 \text{ cm}^2$ at the field centre was selected to obtain the mean pixel value. Judicious selection of the ROI allowed for avoidance of possible film artefacts due to the cutting of the film at the film edge, hence reducing the noise and uncertainty of inter-film readings. The responses after the images were read by the ImageJ software were recorded in Table 4.1. These values were plotted to give a calibration function as shown in Figure 4.1.

3.2.2 Planning Computed Tomography

Rando Alderson female anthropomorphic phantom was used in this study (Fig 3.3). The phantom was scanned with a Siemens Emotion CT scanner (Siemens AG, Munich, Germany) with 5 mm slice width and centre–centre spacing. The images from the CT simulator were then exported to the Oncentra Master Plan treatment planning system (TPS), version 4.3 for 3D conformal external beam planning. The Oncentra master plan TPS was used for delineation of planning target volume. The anthropomorphic phantom was irradiated according to the treatment plan, with the EBT2 film positioned on the phantom in the medial and lateral positions. The films were cut according to the contour of the phantom body. After the exposure, the films were digitized and analysed using ImageJ.

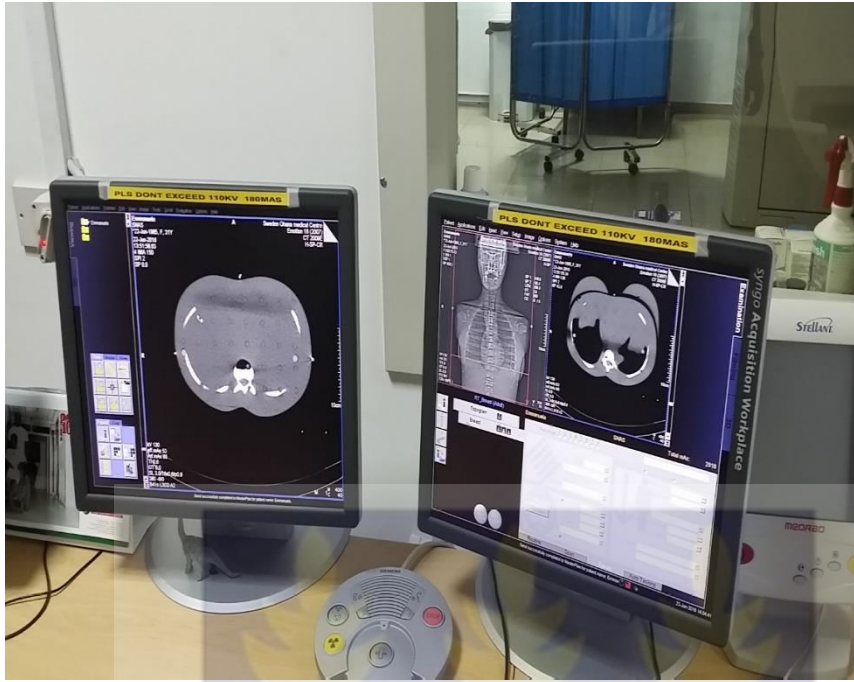


Plate 3. 5: Images of CT scan of the Rando Alderson female anthropomorphic phantom

3.2.3 Treatment planning

Oncentra Master Plan version 4.3 was utilized in the contouring and treatment planning procedures. The left breast case was investigated in this study, so the phantom's right breast was the treated target. The TBV was prescribed to receive a daily dose of 2 Gy per fraction to a total of 50 Gy using 6 MV and 15 MV photons. The target breast volume (TBV) was designed to encompass the volume that was best bounded by CT markers indicating the clinical borders of the breast, the breast contour as it appeared on CT, and the thorax wall. The contours of skin surface, lung and heart were also delineated. Optimal delineation of OAR is crucial since the treatment planning evaluation could be affected. Treatment plans for 3D conformal techniques were simulated for Rando Alderson female anthropomorphic phantom using a 3D TPS. Virtual simulations were performed using a CT-simulator. The CT scan data and plan parameters were exported to the Oncentra Master Plan treatment planning system

(TPS). The treatment plans were delivered on Elekta Synergy 11 linear accelerator, using a 6 MV and 15MV photon beams. Dose calculations for treatment planning were performed by the enhanced Collapsed Cone (CC) convolution algorithm (Oncontra MasterPlan v4.3). A standard tangential plan consisting of medial and lateral fields with aligned posterior field borders was made. Wedges were used to achieve a homogeneous dose distribution inside the CTV. Two opposing coplanar tangential fields with varying segments were organized for the field arrangement to give uniform whole breast irradiation.

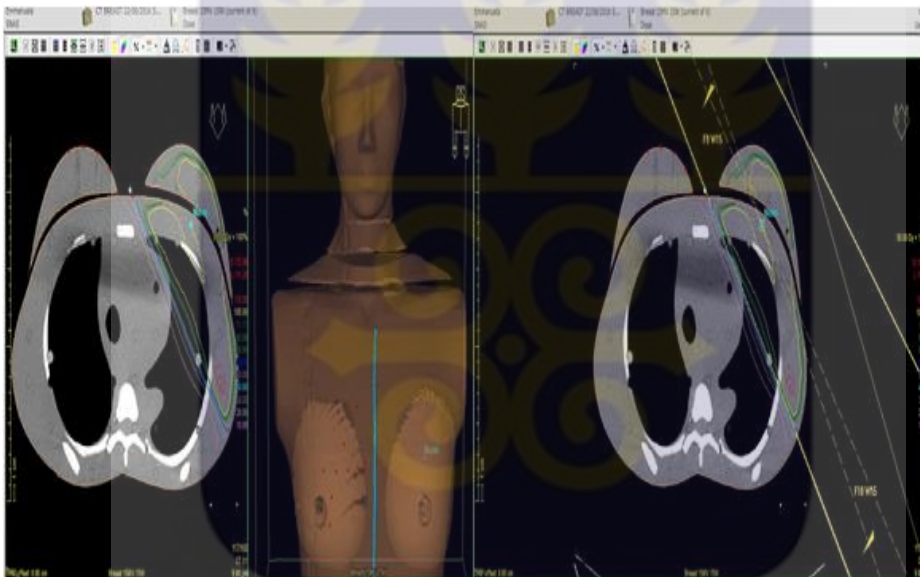


Plate 3. 6: Dose distribution in two tangential wedge field technique

3.2.4 Measurement of contralateral breast dose using Gafchromic EBT2 film.

3.2.4.1 Setup and film irradiations.

Gafchromic films were utilized as the detectors for measuring dose inside the anthropomorphic female Rando phantom. For the contralateral breast dose measurement, the treatment plans were delivered using Elekta Synergy 11 platform linear accelerator equipped with a MLC. On the treatment couch, the Rando phantom

was positioned identical to the CT setups. Sixty Gafchromic EBT2 film detectors were used to measure doses absorbed by the phantom's right breast at different locations, and they were classified into six groups, named A1-9, B1-9, C1-9, D1-9, E1-9 and F1-9. Group A, B and C measured the medial lateral and superior inferior doses for the 6 MV photon beam using MW (15°), MW (30°) and MW (60°) respectively. Group D, E, and F measured the medial lateral and superior inferior doses for 15 MV photon beam using MW (15°), MW (15°) and MW (15°) respectively. The Gafchromic films were placed 2 cm apart on the contralateral breast of the phantom as demonstrated in Figure 3.7. A prescription dose of 2 Gy was delivered to the treated breast by the treatment planning system, and the doses measured by the detectors on the contralateral breast were recorded accordingly. The gantry angles, collimator angles and SSD were kept constant in all the plans.

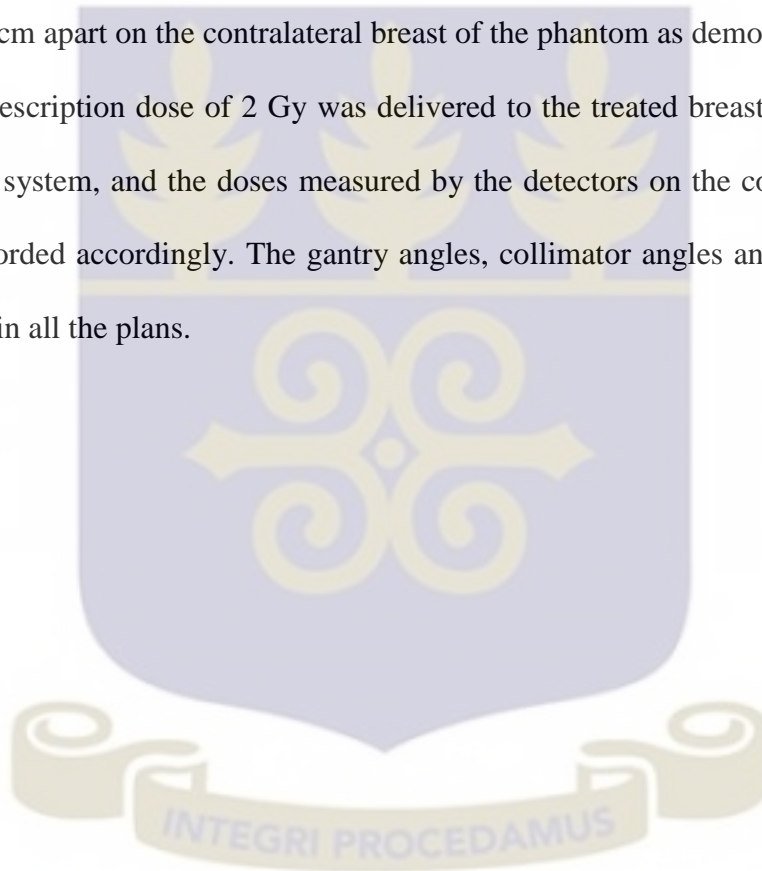




Plate 3. 7: Phantom and Gafchromic film setup for measurement of the doses on the contralateral breast

3.2.4.2 Scanning of irradiated dose films

The EBT2 films were scanned using ScanMaker 9800XL plus 24 hours after irradiation. This was to allow for maximum post irradiation coloration [20]. To maintain the scanning position, a film frame was made and was placed on top of the scanner bed. Scanning orientation was kept consistent for all films. This is because EBT2 film exhibits a different response in portrait orientation compared to the response in landscape orientation of 7%–9% [30]. The films were scanned in transmission mode, 48 bit colour with two separate spatial resolutions of 75 and 300 dpi. All the films in this study were scanned using the same scanner with the same setting and under the

same condition of temperature and humidity on the same day to minimize the scanner variability.

3.2.4.3 Reading of the exposed films.

The exposed films from the 6 MV Elekta Synergy linear accelerator were read using the ImageJ v1.45s by splitting the film image data into red, green, and blue colour channels. For each scanned image and colour channel, a region of interest (ROI) of $3.4 \times 5.0 \text{ cm}^2$ at the field centre was selected to obtain the mean pixel value. Judicious selection of the ROI allowed for avoidance of possible film artefacts due to the cutting of the film at the film edge, hence reducing the noise and uncertainty of inter-film readings. The response values (grey values) after the images were read by the ImageJ software were recorded and using the calibration equation 4.1, these readings were converted to doses as shown in Table (4.2-4.7). The percentage contralateral breast dose were determined for MW (15°), MW (30°) and MW (60°). The same procedure was carried out for the 15 MV photon. The results are found in chapter four.



CHAPTER FOUR

RESULTS AND DISCUSSION

4.0 Introduction

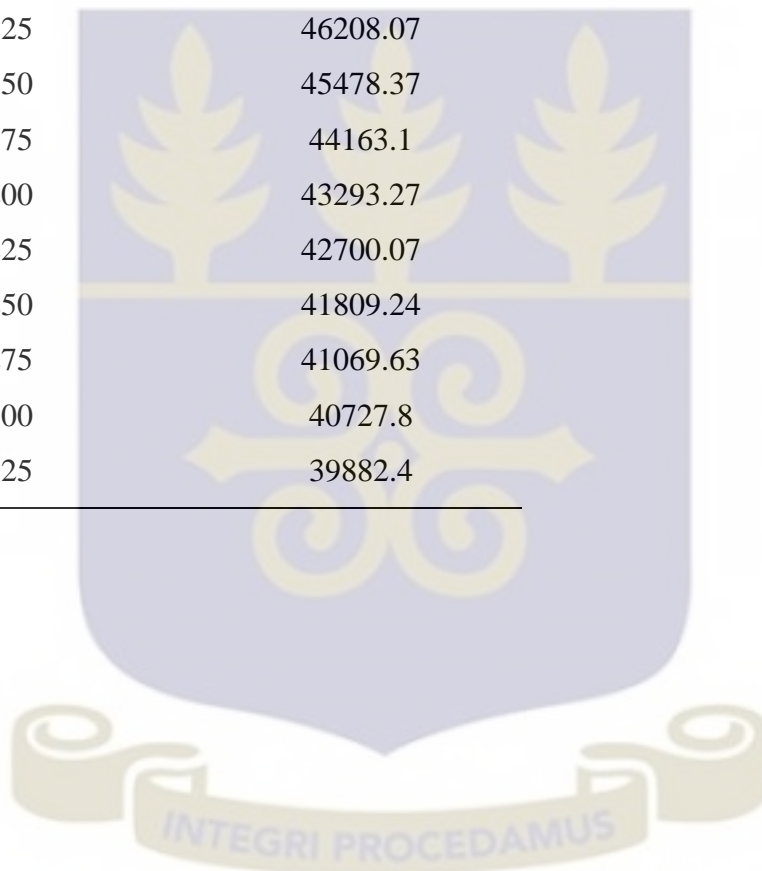
In this chapter, the results from the study are presented and discussed. The study considered the estimation of contralateral breast dose for tangential breast irradiation and 3D CRT techniques using Gafchromic EBT2 films. A discussion of the measured doses and the calculated percentage contralateral breast doses are presented in this chapter.

4.1 Calibration curve

Determining the dose response of Gafchromic EBT2 film is an important step in utilizing these films in dose determination. A calibration curve was constructed using fourth – order polynomial fit to the data. For film set A, three readings of exposed films were recorded and their average values calculated as shown in Table 4.1 below. The corresponding calibration curve is shown Figure 4.1 below.

Table 4. 1: Irradiation of Gafchromic films with 6 MV photons scanned and read out by the ScanMaker 9800XL plus and ImageJ software v1.45s

Dose (cGy)	Grey value ($\pm 0.1\%$)
0	57728.24
25	53586.87
50	51275.21
75	49150.21
100	47672.14
125	46208.07
150	45478.37
175	44163.1
200	43293.27
225	42700.07
250	41809.24
275	41069.63
300	40727.8
325	39882.4



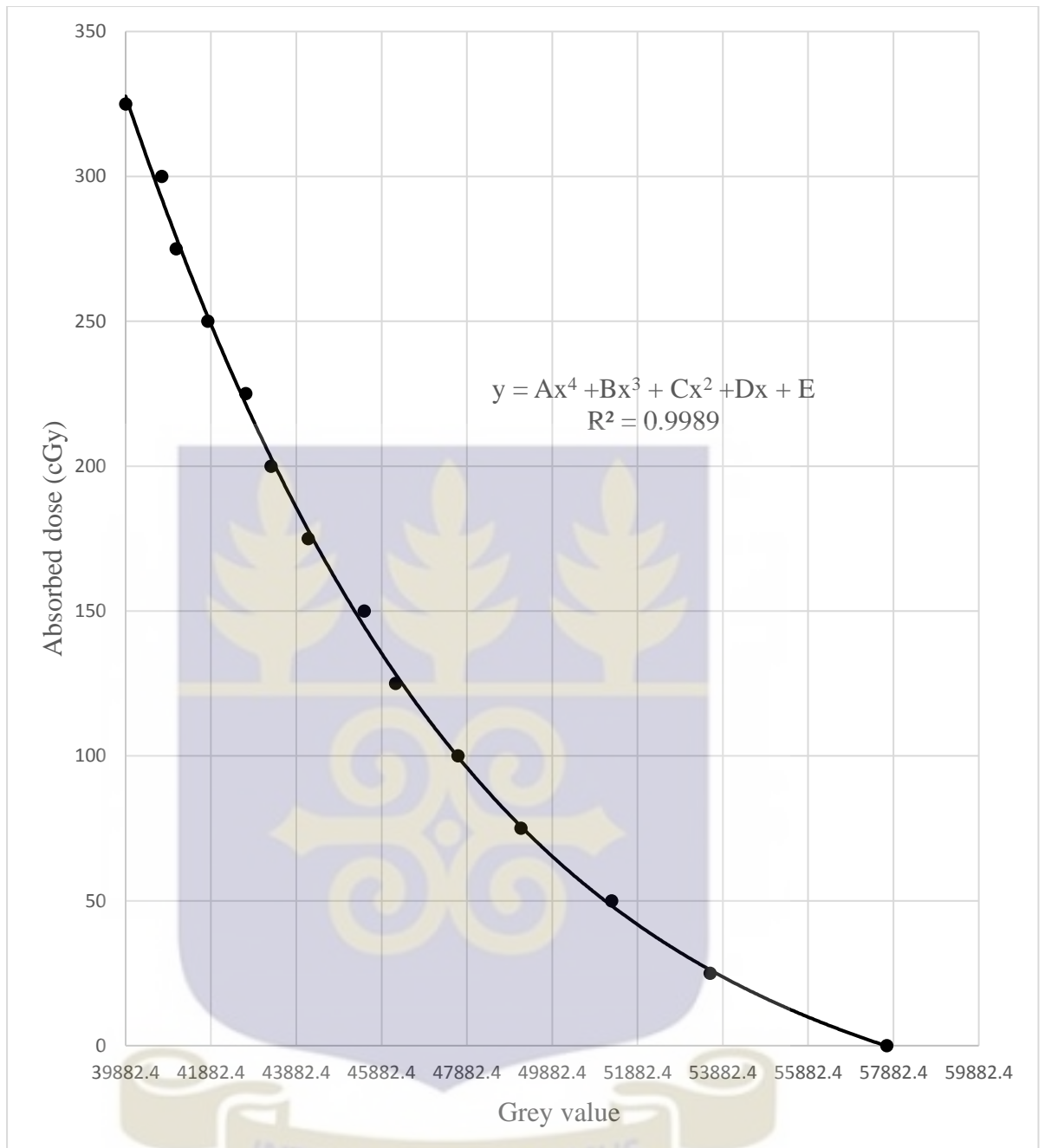


Figure 4. 1: Calibration curves of EBT2 films read out using ImageJ software

A calibration equation obtained from the graph above is given as:

$$y = Ax^4 - Bx^3 + Cx^2 - Dx + C \dots\dots\dots 4.1$$

Where A = 6E-16, B = -2E-10, C = 1E-05, D = -0.6477, E = 10807 and R-square value is 0.9991. The grey values were converted into doses using equation 4.1 above.

4.2 Results

The readings recorded by each Gafchromic film detector represented the contralateral breast dose for single fraction. To convert the measured values to the dose for entire course of treatment delivering 50 Gy to the treated breast, the readings were multiplied by 25 to get the total dose.

Table 4. 2: Measured contralateral breast dose for 6 MV using MW (15°)

Dose point label	Dose(Gy/fraction)	Total dose(Gy)	% dose (Gy)
DP1 ML	0.22	5.50	11.00
DP2 ML	0.15	3.75	7.50
DP3 ML	0.07	1.75	3.50
DP4 ML	0.03	0.75	1.50
DP5 ML	0.01	0.25	0.50
DP6 SI	0.01	0.25	0.50
DP7 SI	0.07	1.75	3.50
DP8 SI	0.05	1.25	2.50
DP9 SI	0.04	1.00	2.00
Total	0.65	16.25	32.50
	mean dose ($\pm 2\%$)	1.81	3.61



Table 4. 3: Measured contralateral breast dose for 6 MV using MW (30°)

Dose point label	Dose(Gy/fraction)	Total dose(Gy)	% dose (cGy)
DP1 ML	0.24	6.00	12.00
DP2 ML	0.15	3.75	7.50
DP3 ML	0.09	2.25	4.50
DP4 ML	0.03	0.75	1.50
DP5 ML	0.02	0.50	1.00
DP6 SI	0.01	0.25	0.50
DP7 SI	0.07	1.75	3.50
DP8 SI	0.06	1.50	3.00
DP9 SI	0.03	0.75	1.50
Total	0.70	17.50	35.00
mean dose ($\pm 2\%$)		1.94	3.89

Table 4. 4: Measured contralateral breast dose for 6 MV using MW (60°)

Dose point label	Dose(Gy/fraction)	Total dose(Gy)	% dose (cGy)
DP1 ML	0.23	5.75	11.50
DP2 ML	0.16	4.00	8.00
DP3 ML	0.10	2.50	5.00
DP4 ML	0.08	2.00	4.00
DP5 ML	0.03	0.75	1.50
DP6 SI	0.01	3.75	7.50
DP7 SI	0.07	1.75	3.50
DP8 SI	0.04	1.00	2.00
DP9 SI	0.02	0.50	1.00
Total	0.74	18.50	44.00
mean dose ($\pm 2\%$)		2.05	4.88

Table 4. 5: Measured contralateral breast dose for 15MV using MW (15°)

Dose point label	Dose(Gy/fraction)	Total dose(Gy)	% dose (cGy)
DP1 ML	0.26	6.50	13.00
DP2 ML	0.19	4.75	9.50
DP3 ML	0.13	3.25	6.50
DP4 ML	0.04	1.00	2.00
DP5 ML	0.02	0.50	1.00
DP6 SI	0.01	0.25	0.50
DP7 SI	0.13	3.25	6.50
DP8 SI	0.16	4.00	8.00
DP9 SI	0.15	3.75	7.50
Total	1.09	27.25	54.50
	mean dose ($\pm 2\%$)	3.03	6.05

Table 4. 6: Measured contralateral breast dose for 15MV using MW (30°)

Dose point label	Dose(Gy/fraction)	Total dose(Gy)	% dose (cGy)
DP1 ML	0.29	7.25	14.50
DP2 ML	0.22	5.50	11.00
DP3 ML	0.13	3.25	6.50
DP4 ML	0.03	0.75	1.50
DP5 ML	0.02	0.50	1.00
DP6 SI	0.01	0.25	0.50
DP7 SI	0.13	3.25	6.50
DP8 SI	0.16	4.00	8.00
DP9 SI	0.15	3.75	7.50
Total	1.14	28.50	57.00
	mean dose ($\pm 2\%$)	3.16	6.33

Table 4. 7: Measured contralateral breast dose for 15MV using MW (60°)

Dose point label	Dose(Gy/fraction)	Total dose(Gy)	% dose (cGy)
DP1 ML	0.31	7.75	15.50
DP2 ML	0.22	5.50	11.00
DP3 ML	0.13	3.25	6.50
DP4 ML	0.06	1.50	3.00
DP5 ML	0.02	0.50	1.00
DP6 SI	0.01	0.25	0.25
DP7 SI	0.12	3.00	6.00
DP8 SI	0.15	3.75	7.50
DP9 SI	0.14	3.50	7.00
Total	1.16	29.00	57.75
	mean dose ($\pm 2\%$)	3.22	6.42

4.3 Discussion

4.3.1 Measured contralateral breast doses

The treatment techniques employed to treat breast cancer cases have been advancing over the past decades, from the conventional wedged tangential fields to inverse-planned IMRT. Though the dose distribution to the ipsilateral breast is improving, the peripheral dose absorbed by the contralateral breast varies. Several studies have indicated that there has been an increased risk of contralateral breast cancer, particularly in young women treated with radiotherapy [18, 28]. Contralateral breast should be contoured as an organ at risk suggested by the RTOG guideline [27]. The scattered radiation dose is directly correlated with the distance from the scattering object, such as collimators and wedges, to the contralateral breast and also with the identity of the scattering object. The identity of the scattering object includes the sizes of the field-shaping collimators and wedge angles. These features also affect the leakage radiation to the contralateral breast. The quality and quantity of the internally scattered photons

depend on the lateral beam characterized by the wedge angle and field size. Radiation carcinogenesis is a stochastic process where the probability of cancer induction increases with dose and there is no threshold dose therefore the dose to the contralateral breast as a result of radiotherapy of breast should not be ignored particularly in patients younger than 45 years. Many researchers have reported the contralateral breast dose; some reported measurement on patients while some reported measurements on phantom. Gao et al. [15] found a relative risk of 1.32 and 1.15, respectively, for second cancer induction in the contralateral breast of women patients whose ages were below 45 years and over 55 years at the time of diagnosis. In a 15-year follow-up, Obedian et al [26] reported that a 10% increase in contralateral breast cancer rate in patients who had radical mastectomy under the age of 45 and received a total dose of 46-54 Gy to the involved breast. Boice et al [18] have conducted case control study in cohort of 41,109 women diagnosed with breast cancer and analysed the records. Their results showed that the mean dose to contralateral breast was 282 cGy with maximum of 710 cGy. They found that the overall increase in risk of contralateral breast malignancy was 1.19 due to treatment of primary radiation. They concluded that the risk of developing second malignancy in the contralateral breast was significantly high in patients who were treated with radiotherapy at younger age than 45 years for primary breast malignancy. This indicates high risk for younger patients

In this study the contribution of peripheral dose outside the field to the contralateral breast using different motorised wedge angles and different beam energies were compared. Tables (4.2-4.7) above provide the dose measured to the contralateral breast for each wedge angle and beam energy. The results show that the scattered radiation from the medial wedge contributes a majority of the contralateral breast dose. This is in agreement with the previous researches that the omission of the wedge on the medial

field can greatly reduce the contralateral breast dose [12]. The percentage mean dose to the contralateral breast for 6 MV photon beam using MW (15°), MW (30°) and MW (60°) were 3.61%, 3.89% and 4.88% of the total primary breast dose as demonstrated in Tables (4.2 - 4.3) above. The percentage mean dose to the contralateral breast for 15 MV photon beam using MW (15°), MW (30°) and MW (60°) were 6.05%, 6.33% and 6.42% of the primary breast dose (50 Gy) as demonstrated in Tables (4.5 – 4.7) above. The mean dose to the entire contralateral breast for 6 MV photon beam was 1.81 Gy for MW (15°), 1.94 Gy for MW (30°) and 2.05 Gy for MW (60°) respectively while the mean dose to the entire contralateral breast for the 15 MV photon beam were 3.03 Gy for MW (15°), 3.16 Gy for MW (30°) and 3.22 Gy for MW (60°). These results are in accordance with those reported by Boice et al [18]. They estimated that the mean radiation dose to the contralateral breast was 2.82 Gy (max. 7.10 Gy). Factors that may contribute to the contralateral breast dose include the orientation of the beams and wedges. The RTOB breast study protocol recommends keeping the Dmax of the contralateral breast <3-3.5 Gy [27]. The mean dose to the entire contralateral breast for 6 MV and 15 MV photon beam were 1.93 Gy and 3.13 Gy respectively. These results are within the range recommended by the RTOG breast study protocol.

4.3.2 Effect of beam energy on contralateral breast dose

Analysis of the results shows that the 15MV photon beam produced higher doses to the contralateral breast as compared with the 6 MV photon beam by 6.42%. For the 6 MV photon beam, the mean contralateral breast dose for the MW (15°), MW (30°) and MW (60°) were 3.61%, 3.89% and 4.88% respectively as demonstrated in Table 4.8. Using the same treatment technique for the 15 MV photons the contralateral breast dose for

the MW (15°), MW (30°) and MW (60°) were 6.05%, 6.33% and 6.42% respectively as demonstrated in Table 4.8 and Figure 4.2.

Table 4. 8: Summary of the mean dose to the contralateral breast dose

Energy (MV)	Wedge angle(°)	% mean dose ($\pm 2\%$)
6	15	3.61
	30	3.89
	60	4.88
15	15	6.05
	30	6.33
	60	6.42



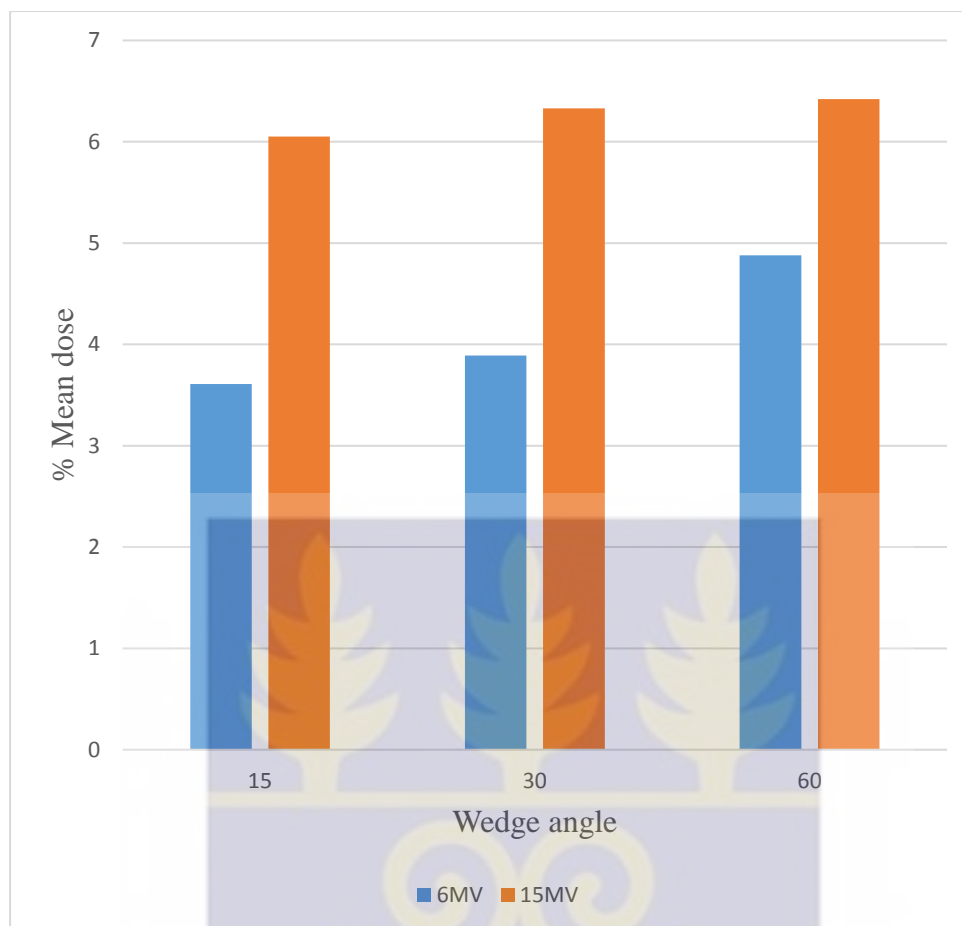


Figure 4. 2: Comparison of beam energy on contralateral breast dose

4.3.3 Effect of wedge (MW) on contralateral breast dose

When wedge is added to a beam, the wedge becomes a scattered radiation source which contributes to the dose outside the primary beam. Results show that the mean dose to the contralateral breast for 6 MV using 60° motorised wedge produced higher surface dose to the contralateral breast than 30° and 15° wedges respectively as shown in figure 4.3. Similarly the mean dose to the contralateral breast for 15 MV using 60° motorised wedge produced higher surface dose to the contralateral breast than 30° and 15° wedges respectively. Analysing the data clearly showed that the dose to the contralateral breast increased slightly with increasing wedge angle as demonstrated in figure 4.3 and 4.4 respectively. This is due to scattered radiation in the wedge filter contributing to doses

outside the field. This observation is in accordance with that recorded by Sohn et al [29]. They performed measurements on 10 patients and on an anthropomorphic phantom. They observed that the scattered dose received by the contralateral breast from a field without wedge is 2/3 times lower than the radiation from a field with wedge.

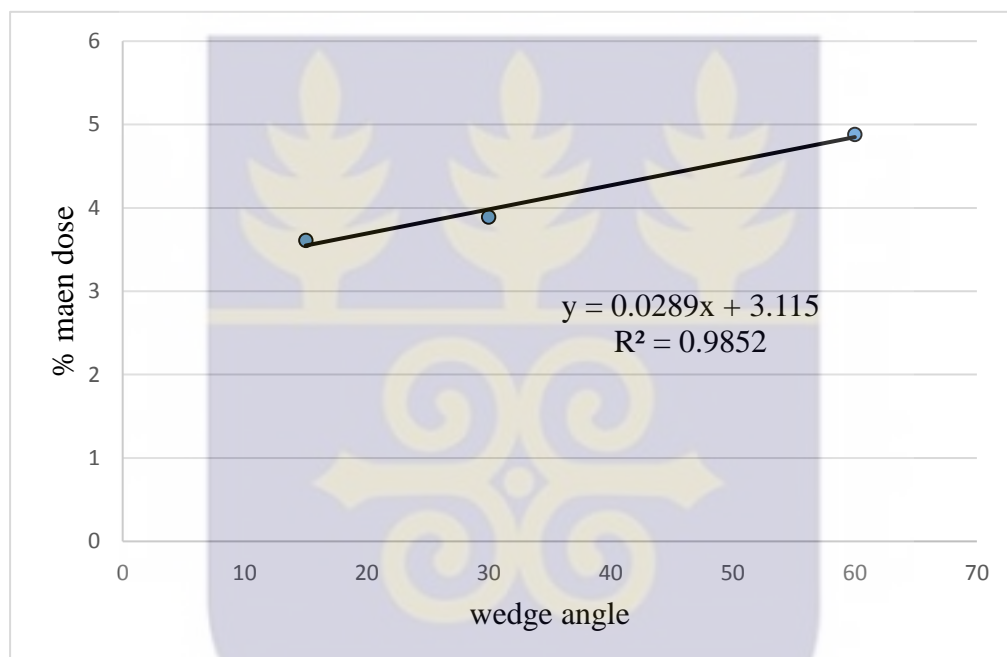


Figure 4. 3: comparison of contralateral breast dose for MW (15°), MW (30°) and MW (60°) using 6 MV photon beam

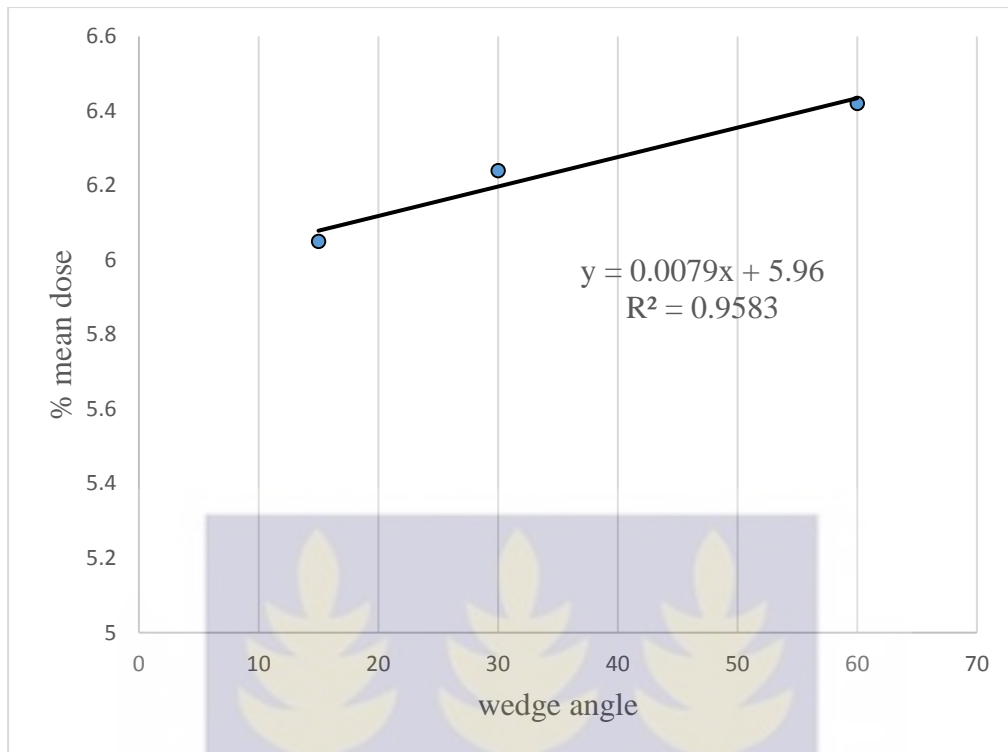


Figure 4. 4: comparison of contralateral breast dose for MW (15°), MW (30°) and MW (60°) using 15MV photon beam



CHAPTER FIVE

CONCLUSION AND RECOMMENDATIONS

5.0. Overview

This chapter contains the conclusions drawn from this study and recommendations on the estimation of dose to the contralateral breast for two tangential wedge fields using Gafchromic films EBT2.

5.1 Conclusion

Complete knowledge of the dosimetric characteristics, including surface and peripheral doses is important for proper choice of a particular wedge system in clinical use. Virtual wedge has clinical benefit which improves the dose distribution in patients undergoing breast conservation.

The dose to the contralateral breast during radiotherapy of breast cancer had been estimated using Gafchromic film EBT2. The EBT2 films were scanned and read using Microtek ScanMaker 9800XL plus and ImageJ software version 1.45s respectively. A calibration curve was constructed and calibration equation was obtained from the graph which was used to convert the grey values into doses. Comparison of the dose to the contralateral breast using different wedge angles and different beam energies were investigated.

Results show that the mean dose to the contralateral breast for 6 MV using 60° motorised wedge produced higher surface dose to the contralateral breast than 30° and 15° wedges respectively. Similarly the mean dose to the contralateral breast for 15 MV using 60° motorised wedge produced higher surface dose to the contralateral breast than 30° and 15° wedges respectively. Results from this study show that the dose to the

contralateral breast increases with increasing wedge angle. Analysis of the results from the 6 MV and 15 MV showed that the 15MV photon beam produced higher doses to the contralateral breast as compared with the 6 MV photon beam by 6.42%.

The results shows that the dose to the contralateral breast increase slightly with increasing wedge angle. This is due to scattered radiation in the wedge filter contributing to doses outside the field.

5.2 Recommendations

The following are the recommendations made to the medical physicists in Sweden Ghana Medical Centre and medical physicists in general

5.2.1. Medical Physicists

Several factors contribute to the contralateral breast dose for tangential treatment of breast. These are photons and electrons scattered externally from the gantry head, collimators, and wedges and photons scattered internally in the body. In order to evaluate the dose to the contralateral breast, scattered beams that vary with the treatment plan need to be considered. The use of wedges increase the scatter dose to the contralateral breast therefore protection of the contralateral breast is necessary when 3DCRT Plus wedges are used. It is not a common practice to use shielding to contralateral breast in local departments. However, to maximize the protection to patients, application of shielding is advisable. It is important that the classic As Low As Reasonably Achievable (ALARA) principle is implemented into clinical practice to minimize scattered radiation received by the contralateral breast and also the surrounding healthy tissues.

5.3 Further study

Further research can be extended to different techniques such as field in field (FIF), tangential fields inverse intensity modulated radiation therapy (T-IMRT). This study used an anthropomorphic Rando phantom as the subject. In future study, to address the limitations of phantom, a group of real patients can be used and dose measurement can be taken in real clinical situations.



REFERENCES

- [1] Podgorsak, E. B., and Podgorsak, M. B. (2005). Special Procedures and Techniques In Radiotherapy. In Radiation Oncology Physics: A Handbook for Teachers and Students. Vienna: International Atomic Energy Agency (IAEA)
- [2] International Commission on Radiation Units and Measurements (1985). Prescribing, recording and reporting photon beam therapy”. Report 50 of ICRU, ICRU Publications.
- [3] International Commission on Radiation Units and Measurements (1999). Prescribing, recording, and reporting photon beam therapy (Supplement to ICRU Report 50)”, ICRU Report 62, ICRU, Bethesda, Maryland, U.S.A.
- [4] GS Sim, JHD Wong, KH Ng (2013). The use of radiochromic EBT2 film for the quality assurance and dosimetric verification of 3D conformal radiotherapy using Microtek ScanMaker 9800XL flatbed scanner
- [5] ISP, (2010). Gafchromic EBT2 dosimetry film manual. White Paper, International Specialty Products, Wayne, New Jersey, USA.
- [6] Sigrun Saur Almberg, Jomar Frengen, L.M.B Fjellsboe_(2009). Contralateral breast doses measured by film dosimetry: Tangential techniques and an optimized IMRT technique *Physics in Medicine and Biology* 54(15):4743-58
- [7] Alzoubi, A. S., Kandaiya, S., Shukri, A., & Elsherbieny, E. (2010). Contralateral breast dose from chest wall and breast irradiation: local experience. *Australasian Physical and Engineering Sciences in Medicine*, 33, 137.

- [8] Sajad A. Rather, M. Mohib-ul Haq, Nazir A. Khan, Ajaz A. Khan, A.G. Sofi (2014). Determining the contralateral breast dose during radiotherapy of breast cancer using rainbow dosimeter
- [9] Mahavir, Singh, & Babita, Jangra (2013). Association between body mass index and risk of breast cancer among females of north India. *South Asian Journal of Cancer*, 3, 121-125.
- [10] Keyvan, Jabbari, Nazli, Azarmahd, Shadi, Babazade, & Alireza, Amouheidari (2013). Optimizing of the tangential technique and supraclavicular fields in 3 dimensional conformal radiation therapy for breast cancer. *Journal of Medical Signals and Sensors*, 3, 107-116.
- [11] Adami, H. O., Bergstrom, R., & Hansen, J. (1985). Age at first primary as a determinant of the incidence of bilateral breast cancer cumulative and relative risks in a population-based case-control study. *Cancer*, 55, 643-647.
- [12] Frass, B. A., Roberson, P. L., & Lichter, A. S. (1985). Dose to the contralateral breast due to primary irradiation. *International Journal of Radiation Oncology Biology Physics*, 11, 485-497.
- [13] Kelly, C., Wang, X., Chu, J., & Hartselle, W. (1996). Dose to contralateral breast: comparison of four primary breast irradiation techniques. *International Journal of Radiation Oncology Biology Physics*, 34, 727-732.
- [14] Muller-Runkel, R., & Kalokhe, U. P. (1990). Scatter dose from tangential breast irradiation to the uninvolved breast. *Radiology*, 175, 873-876.
- [15] Gao X, Fisher SG, Emami B (2003). Risk of second primary cancer in the contralateral breast in women treated for early-stage breast cancer: A population-

based study. *International Journal of Radiation Oncology Biology Physics*. 2003; 56: 1038-1045.

[16] Hill-Kayser CE, Harris EER, Hwang W-T, Solin LJ (2006). Twenty-year incidence and patterns of contralateral breast cancer after breast conservation treatment with radiation. *International Journal of Radiation Oncology Biology Physics*. 2006; 66: 1313-1319.

[17] Stovall M et al (2008). Dose to the contralateral breast from radiotherapy and risk of second primary breast cancer in the WECARE study. *International Journal of Radiation Oncology Biology Physics*. 2008; 72: 1021-1030.

[18] Boice JD, Harvey EB, Blettner M, et al (1992). Cancer in the contralateral breast after radiotherapy for breast cancer. *N Engl J Med*. 1992;326:781–5.

[19] Azam Niroomand-Rad, Chair Charles Robert Blackwell, Bert M. Coursey (1988). Radiochromic film dosimetry: Recommendations of AAPM Radiation Therapy Committee Task Group 55: Reprinted from *medical physics*; Vol.25, Issue 11.

[20] Cheung T, Butson MJ, Yu PKN (2005). Post-irradiation colouration of Gafchromic EBT radiochromic film. *Phys Med Biol*. 2005;50(20):N281–N5.

[21] IAEA International Atomic Energy Agency (2008) .Transition from 2-D Radiotherapy to 3-D Conformal and Intensity Modulated Radiotherapy, IAEA-TECDOC-1588, IAEA, Vienna.

[22] A. Aydarous (2014). Measurement and Comparison of Skin Dose Distribution in Water Phantom Exposed to 6 MV Photon Beam. *Journal of Applied Sciences*, 2014:14: 1952-1958.

- [23] Scalzetti E.M, Huda W, Bhatt S, Ogden K.M (2008). A method to obtain mean organ dose in a Rando phantom. *Health physics*, 2008;95:241-244
- [24] McCredie JA, Inch WR, Alderson M (1975). Consecutive primary carcinoma of the breast. *Cancer* 1975;35:1472-1477
- [25] Hankey BF, Curtis RE, Naughton MD, Boice JD, Flanney JT (1986). A retrospective analysis of second breast cancer risk for primary breast cancer patients with an assessment of the effect of radiation therapy *J Nat Cancer Inst* 1983;70:797-804
- [26] Obedian, E., Fischer, D. B., & Haffty, B. G. (2000). Second malignancies after treatment of early-stage breast cancer: lumpectomy and radiation therapy versus mastectomy. *Journal of Clinical Oncology*, 18, 2406e2412.
- [27] <http://www.rtog.org/ClinicalTrials/ProtocolTable.aspx> (2011). Accessed 20/11/2011.
- [28] Cumberlin RL, Dritschilo A, Mossman KL (1989). Carcinogenic effects of scattered dose associated with radiation therapy. *Int J Radiat Oncol Biol Phys*. 1989;17:623–9.
- [29] SOHN J. W., et al (1999). A mobile shield to reduce scatter radiation to the contralateral breast during radiotherapy for breast cancer: Preclinical Results. *Int. J. Radiation Oncology Biol. Phys.*, Vol.43, No. 5, pp. 1037–1041
- [30] Andres, C., del-Castillo, A., Tortosa, R., Alonso, D. and R Barquero (2010). A comprehensive study of the Gafchromic EBT2 radiochromic film: a comparison with EBT. *Medical Physics*, 37(12):6271–6278.
- [31] Arjomandy, B., Tailor, R., Anand, A., Sahoo, N., Gillin, M., Prado, K. and Vicic, M. (2010) “Energy dependence and dose response of Gafchromic EBT2 film

over a wide range of photon, electron, and proton beam energies”, *Med. Phys.* 37, 1942-1947.

[32] Blackwell, C. R., Coursey, B. M., Gall, K. P., Galvin, J. M., McLaughlin, W. L., Meigooni, A. S., and Soares, C. G. (1998). *Radiochromic Film Dosimetry* (Vol. 25). United States of America.

[33] Boivin, J., Tomic, N., Fadlallah, B., DeBlois, F. and S Devic (2011). Reference dosimetry during diagnostic CT examination using XR-QA radiochromic film model. *Medical Physics*, 38(9), 5119–5129.

[34] Bortfeld, T (2011). IMRT: a review and preview. *Phys Med Biol*, 51(13): p. R363-79.

[35] Brown, T. A. D., Hogstrom, K. R., Alvarez, D., II, K. L. M., Ham, K., and Dugas, J. P. (2012). Dose-response curve of EBT , EBT2 , and EBT3 radiochromic films to synchrotron-produced monochromatic x-ray beams . *Medical Physics*, 39(12), 7412–7417.

[36] Butson, M. J., Yu, P. K. N., Cheung, T., and Metcalfe, P. (2003). Radiochromic film for medical radiation dosimetry. *Materials Science and Engineering R: Reports*, 41(3-5), 61–120. [http://doi.org/10.1016/S0927-796X\(03\)00034-2](http://doi.org/10.1016/S0927-796X(03)00034-2)

[37] Convery, D. J. and M. E (1992). Rosenbloom, The generation of intensity-modulated fields for conformal radiotherapy by dynamic collimation. *Physics in Medicine and Biology*, 37(6): 1359.

[38] Devic, S (2011). “Radiochromic film dosimetry: Past, present, and future” *Physica Medica* 27, 122-134

[39] Devic, S., Aldelaijan, S., Mohammed, H. and Tomic, N (2010). Absorption spectra time evolution of EBT-2 model GAFCHROMICTM film. *Medical Physics*, 37(5):2207–2214.

- [40] Devic, S. et al., (2005). "Precise radiochromic film dosimetry using a flat-bed document scanner." *Medical Physics*, 2245.
- [41] Evans, M. D. C. (2005). Computerized Treatment Planning Systems for External Photon Beam Radiotherapy. In *System* (pp. 387–406). International Atomic Energy Agency (IAEA).
- [42] Gscheidlen, W. (1959). "Device for collimation of a ray beam" US Patent 2904692.
- [43] Brsthme, A (1985/87)"Multileaf collimator "US Patemno 4672212
- [44] International Atomic Energy Agency (IAEA). (2006). Safety Reports Series No . 47 Radiotherapy Protection in the Design of Radiotherapy Facilities. Vienna.
- [45] International Speciality Products. (2010). Gafchromic® ebt2. 1361 Alps Road Wayne.
- [46] International Speciality Products Gafchromic R EBT2 (2009). Self-developing film for radiotherapy dosimetry, Wayne, NJ, USA.
- [47] Jordan, T. and Williams, P. (1994). "The design and performance characteristics of a multileaf collimator." *Physics in Medicine and Biology* 39, 231-251.
- [48] Kairn, T., Hardcastle, N., Kenny, J. and Meldrum, R (2011). EBT2 radiochromic film for quality assurance of complex IMRT treatments of the prostate: Micro-collimated IMRT, RapidArc, and TomoTherapy. *Australasian Physical & Engineering Science in Medicine*, 34:333–343.
- [49] Robinsohn, I (1906) "Apparat zur radiologischen Belichtung lebender und lebloser Objekte". German patent 192300.
- [50] Martisikova, M., Ackermann, B. and Jakel, O (2008). Analysis of uncertainties in Gafchromic R EBT film dosimetry of photon beams. *Physics in Medicine and*

Biology, 53(24):7013.

[51] Nakano, M., Hill, R. F., Whitaker, M., Kim, J. H., and Kuncic, Z. (2012). A study of surface dosimetry for breast cancer radiotherapy treatments using Gafchromic EBT2 film. *Journal of Applied Clinical Medical Physics / American College of Medical Physics*, 13(3), 3727. <http://doi.org/10.1120/jacmp.v13i3.3727>

[52] Parker, W., and Patrocino, H. (2005). Clinical treatment planning in external photon beam radiotherapy. In *Radiation oncology physics: a handbook for teachers and students...*(pp.179–224). Retrieved from <http://citeseerx.ist.psu.edu/viewdoc/download?>

[53] Richley, L., John, A. C., Coomber, H. and Fletcher, S (2010) Evaluation and optimization of the new EBT2 radiochromic film dosimetry system for patient dose verification in radiotherapy. *Physics in Medicine and Biology*, 55(9):2601.

[54] Sharma S. C. *Beam Modification Devices in Radiotherapy* (2007). SlideShare Website, [Online; accessed July. 6, 2016]. Available from: <http://www.slideshare.net/santam/beam-modification-in-radiotherapy-147021>.

[55] Sutherland J. G, Rogers D. W. (2010). Monte Carlo calculated absorbed-dose energy dependence of EBT and EBT2 film. *Med Phys*. 37(3):1110–16.

[56] The Dosimetry Company, U. (2010). B3 Radiochromic Film Dosimetry.

[57] Thuo, K. K. (2013). *Skin Depth Dose Distribution Measurement and Analysis using Radiochromic Dosimetry*. Oregon State University.

[58] Webb, S. (1993). *The Physics of Three-Dimensional Radiation Therapy, Conformal Radiotherapy, Radiosurgery and Treatment Planning*. Bristol: Institute of Physics (IOP).

[59] Faiz, M.K (2003). *The Physics of Radiation Therapy*, 3rd ed. Philadelphia: Lippincott &Wilkins, pp. 465-474

- [60] Haydaroglu A, Ozyigit G. (2013). Principles and practice of modern radiotherapy techniques in breast cancer. New York: Springer.
- [61] Aebi S, Davidson T, Gruber G, Cardoso F. (2011). Primary breast cancer: ESMO Clinical Practice Guidelines for diagnosis, treatment and follow-up. *Annals of Oncology*.
- [62] Van Asselen B, Raaijmakers C.P.J, Hofman P, Lagendijk J.J.W (2001). An improved breast irradiation technique using three-dimensional geometrical information and intensity modulation. *Radiotherapy and Oncology*; 58: 341-347.
- [63] Bucci MK, Bevan A, Roach M (2005). Advances in radiation therapy: Conventional to 3D, to IMRT, to 4D, and beyond. *CA: A Cancer Journal for Clinicians*; 55: 117-134.
- [64] Aref. A. et al (2000). Dosimetric improvements following 3D planning of tangential breast irradiation. *International Journal of Radiation Oncology Biology Physics*; 48: 1569-1574.
- [65] Mundt AJ, Roeske JC (2005). Intensity modulated radiation therapy: A clinical perspective. Hamilton: BC Decker.
- [66] Webb S (2003). The physical basis of IMRT and inverse planning. *The British Journal of Radiology*. 76: 678-689.
- [67] Stern RL (1999). Peripheral dose from a linear accelerator equipped with multileaf collimation. *Medical Physics*. 26: 559-563.
- [68] Mazonakis M, Zacharopoulou F, Varveris H, Damilakis J (2008). Peripheral dose measurements for 6 and 18MV photon beams on a linear accelerator with multileaf collimator. *Medical Physics*. 35: 4396-3403.

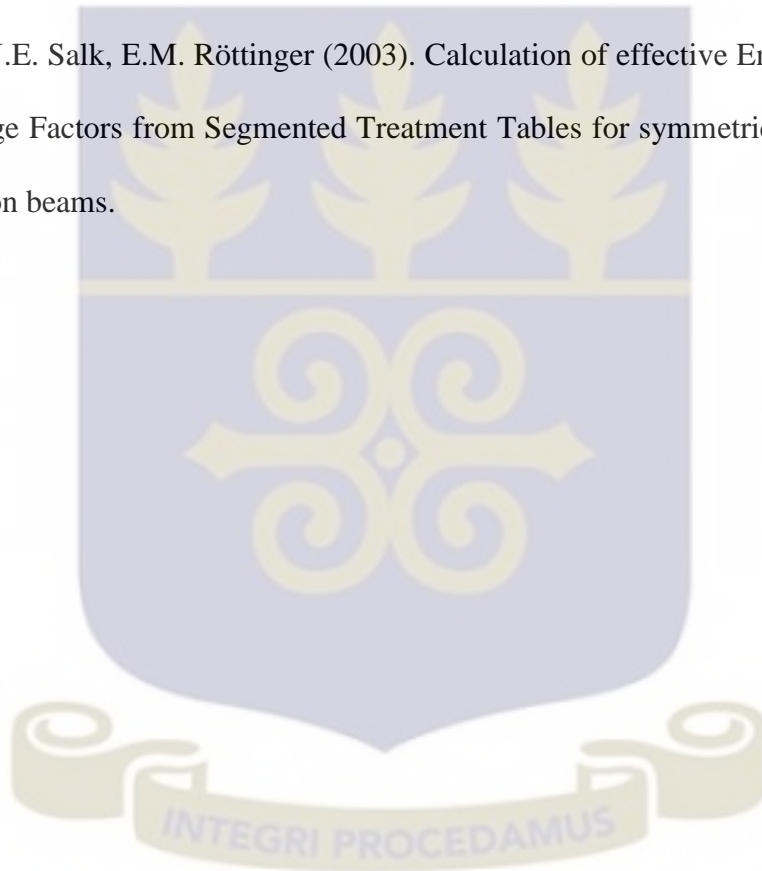
- [69] Tubiana M, Aurengo A, Averbeck D, Masse R (2006). Recent reports on the effect of low doses of ionizing radiation and its dose-effect relationship. *Radiation and Environmental Biophysics*. 44: 245-251. 89.
- [70] Li XA, Tai A, Arthur D.W, et al (2009). Variability of target and normal structure delineation for breast cancer radiotherapy: an RTOG Multi-Institutional and Multi-observer Study. *Int J Radiat Oncol Biol Phys*. 73:944–51.
- [71] Avadhani JS, Pradhan AS, Sankar A, Viswanathan PS (1997). Dosimetric aspects of physical and dynamic wedge of Clinac 2100C linear accelerator. *Strahlentherapie Und Onkologie*.173: 524-528.
- [72] Li Z, Klein E.E (1997). Surface and peripheral doses of dynamic and physical wedges. *International Journal of Radiation Oncology Biology Physics*. 37: 921-925.
- [73] Kirova Y.M et al (2007). Risk of second malignancies after adjuvant radiotherapy for breast cancer: A large-scale, single-institution review. *International Journal of Radiation Oncology Biology Physics*. 68: 359-363.
- [74] Bhatnagar, A. K., Heron, D. E., Deutch, M., Brandner, E., Andrew, W. U., & Kalnicki, S. (2006). Does breast size affect the scatter dose to ipsilateral lung, heart or contralateral breast in primary irradiation using intensity modulated radiotherapy (IMRT). *American Journal of Clinical Oncology*, 29, 80-84.
- [75] Hill-Kayser C.E, Harris EER, Hwang W-T, Solin L.J (2006). Twenty-year incidence and patterns of contralateral breast cancer after breast conservation treatment with radiation. *International Journal of Radiation Oncology Biology Physics*. 66: 1313-1319.
- [76] Hall E.J, Giaccia A.J (2006). *Radiobiology for the radiologist*. 6th ed. Philadelphia: Lippincott Williams & Wilkins.

[77] P. Cherry, A. Duxbury (1998). Practical radiotherapy physics and equipment, 139. Cambridge University Press

[78] Jagsi R, Moran J, Marsh R, et al (2010). Evaluation of four techniques using intensity-modulated radiation therapy for comprehensive locoregional irradiation of breast cancer. *Int J Radiat Oncol Biol Phys.* 78: 1594–603.

[79] Hong L, Hunt M, Chui C, et al (1999). Intensity-modulated tangential beam irradiation of the intact breast. *Int J Radiat Oncol Biol Phys.* 44: 1155–64.

[80] J.E. Salk, E.M. Röttinger (2003). Calculation of effective Enhanced Dynamic Wedge Factors from Segmented Treatment Tables for symmetric and asymmetric photon beams.



APPENDIX

Table A. 1: Percentage error in calibration function in Figure 4.1

Prescribed dose (cGy)	Grey value	Measured Dose (cGy)	Difference (cGy)	% Difference
25	55884.96	26.727	1.727	6.91
50	53534.34	52.032	2.032	4.06
75	51378.83	73.991	-1.009	1.35
100	49912.12	98.753	-1.247	1.25
125	48517.44	128.781	3.781	3.02
150	47518.2	147.569	-2.431	1.62
175	46128.52	177.989	2..989	1.08
200	44994.6	204.781	4.781	2.39
225	44436.53	229.110	4.110	1.82
250	43709.95	252.012	2.012	0.80
275	43113.22	273.113	-1.887	0.69
300	42510.74	298.998	-1.002	0.33
325	41851.81	328.215	3.215	0.99
% mean error				2.02



Table A. 2: Irradiation of Gafchromic films with 6 MV photons scanned and read out by the ScanMaker 9800XL plus and ImageJ software v1.45s

dose (cGy)	Grey value			Average	% Deviation
	Reading 1	Reading2	Reading 3	Reading	
0	57652.21	57821.8	57710.7	57728.24±86.14	0.15
25	53611.11	53642.31	53507.2	53586.87±70.74	0.13
50	51257.62	51266.7	51301.3	51275.21±23.05	0.04
75	49134.8	49102.6	49213.22	49150.21±56.90	0.12
100	47712.71	47605.3	47698.41	47672.14±58.33	0.12
125	46197.5	46209.2	46217.5	46208.07±10.05	0.02
150	45438.1	45496.32	45500.7	45478.37±34.95	0.08
175	44184.7	44217.4	44087.21	44163.1±67.73	0.15
200	43309.1	43279.4	43291.3	43293.27±14.95	0.03
225	42620.9	42689.5	42789.8	42700.07±84.94	0.12
250	41818.7	41771.31	41837.7	41809.24±34.19	0.08
275	41082.6	41105.2	41021.1	41069.63±43.52	0.11
300	40715.4	40778.7	40689.3	40727.8±45.97	0.11
325	39970.3	39789.2	39887.7	39882.4±90.67	0.23
Percentage mean deviation					0.11

